Wind erosion response to past and future agro-pastoral trajectories in the Sahel (Niger)

C. Pierre, P. Hiernaux, Jean-Louis Rajot, L. Kergoat, N. Webb, A. Abdourhamane Touré, B. Marticorena, Christel Bouet

Wind erosion response to past and future agro-pastoral trajectories in the Sahel (Niger)

Pierre C.[1*], Hiernaux P.[2], Rajot JL.[1,3], Kergoat L.[4], Webb N.P.[5], Abdourhamane Touré A.[6], Marticorena B.[7], Bouet C.[1,3]

[1] IEES-Paris (Institute of Ecology and Environmental Sciences - Paris), CNRS, Sorbonne Université, Université Paris Est Créteil, Université de Paris, INRAE, IRD, 4 place Jussieu, 75005 Paris, France, +33 1 44 27 32 96
ORCID : 0000-0002-7549-1460
caroline.pierre@upmc.fr
[*] *corresponding author*

[2] Pastoc, 30 chemin de Jouanal, 82160 Caylus, France
pierre.hiernaux2@orange.fr

[3] Université de Paris and Univ Paris Est Creteil, CNRS, LISA, F-75013 Paris, France
jeanlouis.rajot@ird.fr
christel.bouet@ird.fr

[4] GET (Géosciences Environnement Toulouse), CNRS, Université de Toulouse, IRD, 14 Avenue Edouard Belin, 31400 Toulouse, France
laurent.kergoat@get.omp.eu

[5] USDA-ARS Jornada Experimental Range, Las Cruces, NM, USA
nwebb@nmsu.edu

[6] Université Abdou Moumouni, Faculté des Sciences et Techniques, Département de Géologie, BP 10662 Niamey, Niger
abdourahamane.toure@ird.fr ; doudu2000@yahoo.fr;

[7] Univ Paris Est Creteil and Université de Paris, CNRS, LISA, F-94010 Créteil, France
beatrice.marticorena@lisa.ipsl.fr

Abstract

Context: Wind erosion plays a major role in land degradation in semi-arid areas, especially in the Sahel. There, wind erosion is as sensitive to land use and land management as to climate factors. Future land use intensification may increase wind erosion and induce regional land degradation.

Objective: We aimed to estimate wind erosion responses to changing land management in a Sahelian region.

Methods: We defined land use intensification scenarios for a study site in southwestern Niger for two historical situations (1950s and 1990s), and two alternative prospective scenarios (2030s: extensive or intensive). We simulated vegetation growth and horizontal sediment flux of wind erosion for the corresponding landscapes.

Results: Annual amounts of horizontal sediment flux increased with land management changes from 1950s (nil flux) to 1990s (176 $kg.m^{-1}.yr^{-1}$) and 2030s (452 to 520 $kg.m^{-1}.yr^{-}1$), mostly because of differences in land use, declining soil fertility, and practices decreasing the dry vegetation. For 2030s, intensive scenario exhibited larger vegetation yields than extensive conditions, but similar large values of horizontal sediment flux, thus questioning the sustainability of both scenarios. Realistic sets of practices had as large an influence as the largest theoretical range of practices on the variability of annual horizontal sediment flux. This variability was as large as that due to meteorological conditions.

Conclusions: This study demonstrates that the environmental impact of land use and management practices, of which wind erosion is an aspect, must be assessed at the landscape scale to account for the variability in land cover and associated land management.

Key words: wind erosion; agro-pastoral practices; land management scenarios; land use; modelling; Sahel.

1. Introduction

Unprecedented human population and climate change make it increasingly important to understand soil erosion impacts on the sustainability of socio-ecological systems (*Webb et al.,* 2017). The effects of human-driven land cover change - like grazing intensity, grassland conversion to cropland, crop residue management or ecological restoration programs - on wind erosion has been highlighted in China (*Chi et al.,* 2019; *Du et al.,* 2019; *Zhang et al.,* 2018), in the US (*Duniway et al.,* 2019; *Galloza et al.,* 2018; *Rakkar et al.,* 2019), in Southern (*Webb et al.,* 2020) and Eastern Africa (*Fenta et al.,* 2020) and in the Sahel (*Abdourhamane Toure et al.,* 2019). This issue is critical in semi-arid areas, where environmental conditions are marginal for agriculture and where human-environment interactions can have a large impact on the resilience of farming systems to climate stressors (*IPCC*, 2019). Of these semi-arid areas, the Sahel exhibits the largest population growth, leading to a large food demand, whilst being one of the poorest regions worldwide. Sahelian land degradation is a major concern (*Fensholt et al.,* 2013; *Mbow et al.,* 2015) because Sahelian soils are inherently poor in organic matter and nutrients (*Breman et al,* 2001). In this area, wind erosion plays a major role in land degradation as it can induce annual losses of several millimeters of topsoil (*Sterk*, 2003). The consequent nutrient losses can be of the same order as that needed as uptake for millet growth, the main staple crop in the area (*Sterk*, 2003).

In the Sahel, wind erosion depends on natural factors (wind, rain, vegetation cover) as much as on land management (*Pierre et al.,* 2018). Wind erosion not only depends on land use (e.g. cropland versus rangeland) but also on associated management practices. For a given land use (e.g. cropland), with Sahelian meteorological conditions, wind erosion could vary by as much as a factor of ten (in terms of annual mass of the horizontal sediment flux, see *Pierre et al.,* 2018) depending on management practices. The agro-pastoral practices of local farmers and herders follow risk-avoidance strategies in response to the high variability of Sahelian rainfall, in terms of annual amount as well as event intensity and distribution throughout the rainy season (from June to October approximately). In many agro-pastoral systems, the different practices strongly interact and should thus be considered at the landscape scale. Nutrient transfer to croplands provided by livestock and manure is a good example of such interactions (*Turner and Hiernaux,* 2015). Diversification of resources at the household scale also shapes practices at the landscape scale (*Raynaut*, 2001). As for other dryland cropping systems, cropping practices like choice of crop species and cultivars, sowing date, weeding and management of crop residues can significantly influence wind erosion (*Pierre et al.,* 2018; *Thomas et al.,* 2018). Some of these practices could lead to increased wind erosion and eventually to feedbacks of wind erosion on land health and management through decline in soil fertility or reactivation of dunes (*Tidjani et al.,* 2009).

As stated by *Lavigne-Delville* (1997), cited by *Warren et al.* (2001): "*soil degradation can only be understood in its social context*." According to these authors (*Warren et al.,* 2001), who relied on a "local political ecology" approach, soil erosion in southwestern Niger can be related to socio-economic factors like male migration and access to non-farm incomes. However, observations and quantitative evidence of these interactions are scarce. Wind erosion affects soil fertility over the long-term and thus is not necessarily perceived as an urgent threat by local farmers; this could hinder short-term prevention of wind erosion by local populations, although soil fertility is one of their main concerns (*Warren et al.,* 2003).

Despite the influence of wind erosion on the sustainability of Sahelian agro-pastoral systems, no studies have quantified the interactions among changing land use, agro-pastoral practices and erosion rates in the Sahel. No information on land management has been recorded alongside available classifications of Sahelian land use systems to support such analyses (e.g. *Klein Goldewijk et al.,* 2011; *Monfreda et al.,* 2008; *Tappan et al.,* 2016). Furthermore, little is known about cropland change and land management dynamics at the Sahel-scale (*van Vliet et al.,* 2013). It is therefore challenging to define realistic scenarios of past and future Sahelian land use and agro-pastoral practices, along with associated socio-ecological changes, to evaluate their impacts on wind erosion and its influence on the sustainability of Sahelian agro-pastoral systems. Recent research based on field measurements (*Pierre et al.,* 2014, 2015), model-driven sensitivity analysis (*Pierre et al.,* 2018) and survey of land management and vegetation production (e.g. *Hiernaux et al.,* 2009) provide a basis for developing such scenarios to assess land use and management practices impacts on wind erosion, and to establish a foundation for future systems-level research to address land degradation-climate change interactions.

Here we investigate the impact of past and future trajectories of Sahelian agro-pastoral practices on wind erosion. We develop landscape-level land use strategies and trajectories as scenarios based on expert knowledge and published literature for a case study in southwestern Niger. Using a set of models developed in previous work, we then investigate the impact of the scenarios on wind erosion. The spatial extent of our study site is about 30 km x 30 km, the scale at which land use activities reflect decision-making at the rural community level. This scale also approximates one grid cell for Earth System models (e.g. *Pierre et al.,* 2012), thus investigation at this scale could help address how local-scale heterogeneity in land use and management affecting wind erosion influences regional dust emissions. Section 2 introduces the selected study site and defines the scenarios of practices, before describing the modelling approach. Section 3 presents the results of vegetation and wind erosion simulations and analyzes the impact of practices scenarios on these variables. The results are discussed in section 4; section 5 gathers the main conclusions of the study.

2. Materials and Methods

2.1. Study site

The study area is a 30 km x 30 km extent in the Fakara district, within the Tillaberi administrative region in southwestern Niger, about 75 km east of the capital, Niamey (*Figure 1*). The Fakara district is located between confluent valleys of the Niger River to the West and the fossil valley of Dallol Bosso to the East. The annual rainfall is typical of Sahelian conditions with currently about 500 mm per year (e.g. *Marticorena et al.,* 2017), with a narrow unimodal distribution (June to September) due to the African monsoon. About 20% of the area is covered by shallow loamy sand soils on flat hard pan plateaus, not prone to wind erosion because of soil crusts and tiger bush vegetation cover. Deep sandy soils dominate largely the rest of the landscape, with loamy-clay soils limited to the narrow ephemeral river bed and pond floor, i.e. less than 5% of the landscape area (*Turner and Hiernaux,* 2015). We restrict our analysis to the arable sandy soils (~80% of the area), considering that the remaining 20% are not prone to wind erosion.

The study area has been a focal point for research over the last decades, including accounts of meteorological and soil conditions and land use and land management practices (e.g. *Goutorbe et al.,* 1997; *Warren et al.,* 2003; *De Rouw and Rajot,* 2004; *Cappelaere et al.,* 2009; *Hiernaux et al.,* 2009). Several field measurements were dedicated to the dynamics of wind erosion (*Rajot*, 2001; *Bielders et al.,* 2004), some of which included the monitoring of crop residue degradation and land use effects (*Abdourhamane Toure et al.,* 2011). Measurements of meteorological data and dust concentration and deposition fluxes were also collected since 2006 (*Marticorena et al.,* 2010, 2017).

The human population in the study area is mainly composed of Jerma people with a strong minority of Fulani, who are respectively farmers and pastoralists, with a recent conversion of the latter to agro-pastoralism. Some minor groups of Kel Tamacheq and Maouri also live in the area (*Hiernaux and Ayantunde*, 2004). Historical land rights for cropping are recognized to Jerma people in Dantiandou, and to Fulani in Birni Ngaoure. The local land use evolved from very slight human impact in the 1950s to cropping, fallowing and livestock grazing in the 1990s and ongoing cropland expansion today, with the major staple-crop being millet (*Pennisetum glaucum*). Over the same period, land management changed with increasing grazing pressure and collection of crop residues (*Schlecht et al.,* 2001; *Akponikpè et al.,* 2014).

As in most parts of the Sahel, wind erosion in southwestern Niger exhibits a large seasonality related to the monsoonal wind and rainfall regimes. Wind erosion occurs when wind speed is large and vegetation cover is low. As the high wind speeds are mostly due to convective systems during the first part of the rainy season (May to July, e.g. *Bergametti et al.,* 2017), a large proportion of the annual wind erosion occurs during this period (e.g. *Abdourhamane Toure et al.,* 2011).

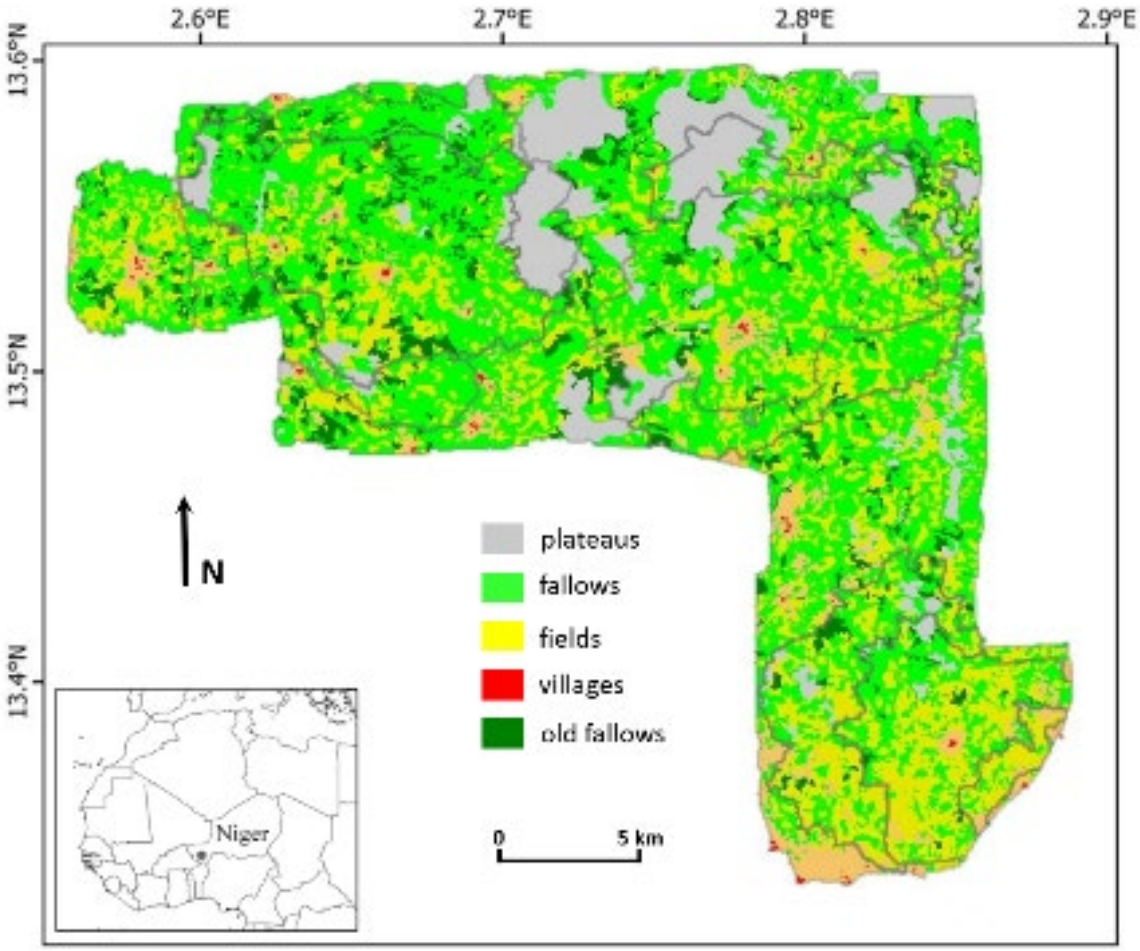

Fig. 1 *Location of the study site and main land uses in 1992*

(adapted from Hiernaux and Ayantunde, 2004)

2.2. Land use and management scenarios

We establish two historical situations and two alternative prospective scenarios that describe evolving land use and land management in the study area, from a *Low density* situation (~1950) to a recent situation (*High density*, ~1990) and to the near future (*Very high density*, ~2030) (*Figure 2*). The historical situations are based on published descriptions of land use trends and on expert knowledge. The prospective scenarios develop two different narratives following a *Very high density, Extensive* pathway, in the line of current practices, and a *Very high density, Intensive* one that is probably more sustainable but requires external inputs. The scenarios are defined as follows (see 2.3 for modelling details):

(i) « Low density (1950s) » situation

Representative of the mid-20th, this scenario assumes a slight human management of the environment, as noticeable recent human settlement in the area started around 1950 (with about 6 inhabitants.km^{-2}) *(Hiernaux and Ayantunde,* 2004). As no permanent water was accessible, the grazing pressure was

slight, limited to the wet season and assumed to have negligible impact on wind erosion (0 TLU.km^{-2}). The land cover is herbaceous savanna over all arable land (i.e. 80% of the landscape).

(ii) « High density (1990s) » situation

This scenario is representative of the 1990s with a more densely populated crop-livestock farming system (about 35 inhabitants.km^{-2}). It combines several land uses and land management practices. Following population increase, cropland area increased significantly since the 1950s. Agro-pastoral practices remain extensive and cultivation implies high time-labor and large cropped areas per household, though limited by labor availability (*Hiernaux and Turner,* 2002). The Jerma and Fulani agrarian cultures transformed into sedentary crop-livestock systems (*Bonfiglioli*, 1990). The development of markets in the large village of Dantiandou and in nearby villages favored cash crops in small gardens (cropped by women), small enough to be neglected for wind erosion analysis. Farming is subsistence-oriented and the dominant crop is millet.

10% of the arable land, located near villages or pastoral camps, is under permanent cropping with livestock manure and house wastes providing nutrients, allowing a large sowing density (10 000 plants.ha^{-1}). The population pressure is still low enough that the remaining 90% of arable land (bush fields) are under shifting cropping systems with fields cultivated for 5 years and fallowed for 3 years to restore soil fertility (*Hiernaux and Turner,* 2002). *Reenberg et al.* (2013) observed similar alternate land use of 5 years cropping and 3 years fallowing on sandy dunes in southeastern Niger after 1984. In these unmanured fields, sowing density is lower (6000 plants.ha^{-1}). In all cultivated fields (manured and unmanured), 10% of crop residues were collected at harvest, as an emerging trend of storing and selling part of these residues.

Thus, for a given year, 8% of the total surface is permanently cropped (10% of the 80% that are arable lands), 45% of the land area is under shifting cultivation ((5/8)*90=56.25% of the arable land) and 27% is fallow ((3/8)*90 = 33.75% of the arable land). The grazing pressure (8 TLU.km^{-2}) is exerted on the whole landscape and corresponds to an equilibrium between livestock density and forage availability in the landscape (see Appendix A).

(iii) « Very high density, Extensive (2030s) » scenario

This scenario intends to be representative of the near future (around 2030), following a narrative in which current agro-pastoral practices are increasingly used. Following the observed recent trends, croplands continue to expand until all arable land is cultivated and no field is fallowed anymore (thus all the landscape but the plateaus). Due to continual nutrient uptake by crops, soil fertility further decreases and farmers adapt planting density to soil fertility (i.e. with lower densities: 4000 plants.ha^{-1}). Livestock are more numerous (12 TLU.km^{-2}) and can still graze on the plateaus during the wet season

and on crop residues during the dry season, but do not necessarily find enough forage on the sandy slopes and valleys of the study area. A large proportion of crop residue (75%) is collected at harvest to feed livestock or to be sold as forage or building material. This estimate aims at representing a large rate of residue harvesting, yet not a total collection, in order to design realistic conditions and not extreme behaviors.

(iv) « Very high density, Intensive (2030s) » scenario

This last scenario is an alternative to what could occur around 2030, assuming funds are available (e.g. from a national policy) to purchase fertilizers and additional animal feed. The association of cropping and livestock is assumed to be maximized and soil fertility is supported with fertilizers. In this case, all arable land is cultivated using manure and inorganic N and P fertilizers and plant densities are large (12 000 plants.ha^{-1}). The fertilizers enhance both grain and stalks/leaf yields and thus fodder resources for livestock, in turn producing more manure. Yet, as in the *Extensive* scenario, livestock (20 TLU.km^{-2}) do not necessarily find enough forage on the sandy slopes and valleys of the study area. A large proportion of crop residue (75%) is collected at harvest and 10% is laid down for surface mulching on crop fields.

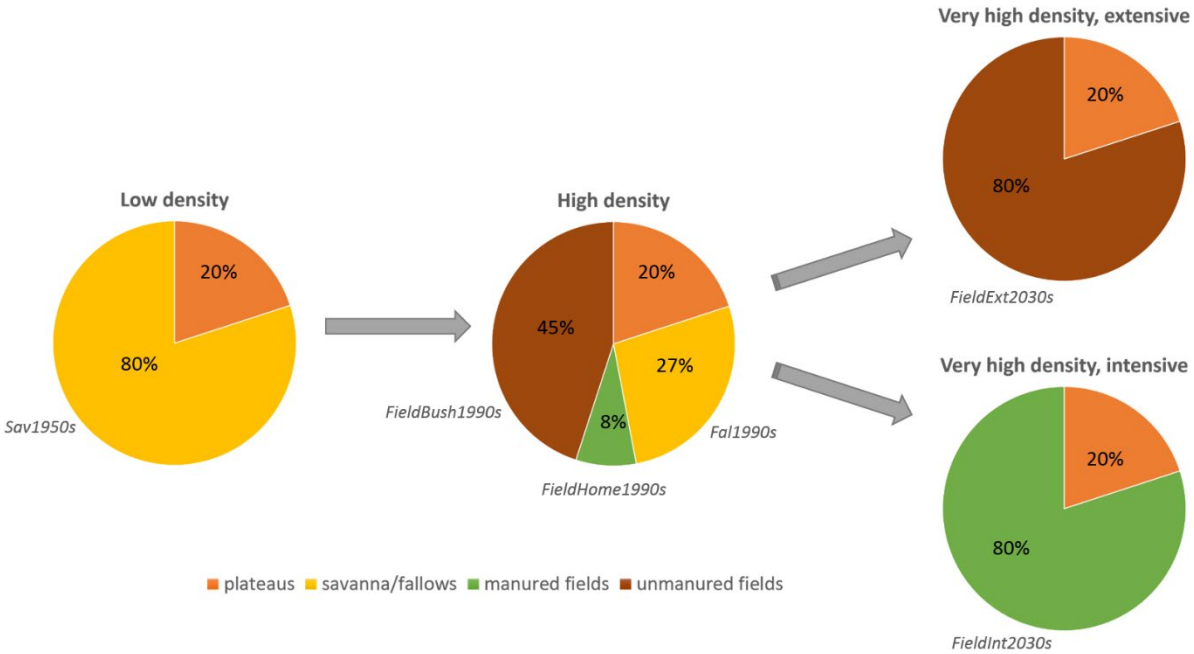

Fig. 2 *Land use proportions depending on the scenarios (with simulation names detailed in 2.3.4). Note that for a given land use, land management can differ: e.g. for savanna/fallows, lower soil fertility for fallows in 'High density' than for savanna in 'Low density'; for unmanured fields, lower plants density and larger residues collecting and grazing pressure in 'Very high density, Extensive' compared to 'High density'; for manured fields, larger soil fertility, plants density, residues collecting and grazing pressure in 'Very high density, Intensive' compared to 'High density' (see Table 2).*

2.3. Models

Wind erosion results from the effect of wind on an unprotected soil surface (i.e. with low or no vegetation cover). It is a threshold phenomenon: the wind has to reach a minimum speed, depending on the surface characteristics, to initiate the movement of soil particles (*Greeley and Iversen,* 1985). Vegetation acts as an obstacle to the wind effect on the surface. Thus, it is essential to characterize the vegetation cover in order to estimate wind erosion. Therefore, we use one model for wind erosion and two models for vegetation cover - one to simulate the herbaceous cover of savanna/fallows and one to simulate millet growth in fields (*Figure 3*).

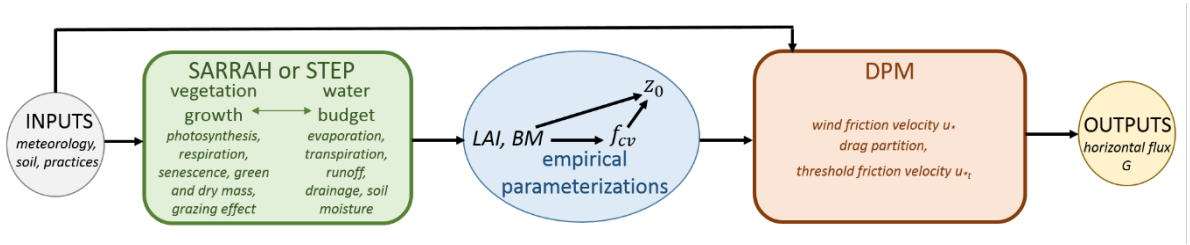

Fig. 3: *Scheme of the models combination. Inputs (meteorological data, soil characteristics, land management practices) drive the vegetation models (SarraH for millet fields, STEP for herbaceous savanna/fallows). Vegetation mass and Leaf Area Index (LAI) enable to estimate surface vegetation cover f_{cv} and aerodynamic surface roughness z_0 using empirical parameterizations. f_{cv} and z_0, along with wind data, drive the wind erosion model to compute the horizontal wind erosion flux G (Figure adapted from Pierre et al., 2015).*

Each scenario depicts a landscape composed of several land units corresponding each to a given land use. For each land unit, simulations of vegetation and horizontal sediment flux were run for the corresponding set of practices (see *Table 2* for the detailed parameters of each simulation). Thus, the spatial scale of the simulations was the scale of a land unit (e.g. a field or a savanna grassland, typically of about 1 ha). The resulting horizontal sediment fluxes were aggregated at the scale of the study area, as the weighed mean of horizontal sediment flux from several land uses i.e. from several model simulations. Transport and spatial redistribution of the horizontal wind erosion flux is not considered here. We briefly describe the models below; more detailed information on equations and parameters of the models can be found in *Pierre et al.* (2015; 2018) and in Appendix B and C.

2.3.1 Wind erosion model

We use here the Dust Production Model (DPM, *Marticorena and Bergametti,* 1995) to estimate wind erosion. This model has provided reliable estimates of the horizontal sediment mass flux at the local scale *(Gomes et al.,* 2003*; Pierre et al.,* 2014) as well as for dust emissions at regional scale *(Laurent et*

al., 2008; *Pierre et al.,* 2012). The DPM estimates horizontal sediment flux *G* as a function of the total wind friction velocity u_* over the vegetated surface and the threshold wind friction velocity u_{*t}, which depends on surface characteristics:

$$G = E\,\frac{\rho_a}{g}\,u_*^3\left(1+\frac{u_{*t}}{u_*}\right)\left(1-\frac{u_{*t}^2}{u_*^2}\right) \text{ if } u_* > u_{*t},\ G = 0 \text{ otherwise} \quad (1)$$

with :

E: proportion of erodible surface (E = 1 – f_{cv} where f_{cv} is the cover ratio of the surface by vegetation)

ρ_a: air density (= 0.001227 g.cm^{-3})

g: gravity (= 981 cm.s^{-2})

The horizontal sediment flux G is expressed in kg.m^{-1} per time unit, i.e. the total mass of particles crossing a 1-m wide vertical plane perpendicular to wind direction with infinite height during the time unit. The drag of the wind on the ground surface is distributed between the soil surface and the vegetation according to a drag partition scheme. In the DPM, the drag partition scheme depends on the surface aerodynamic roughness length z_0, of prime importance for wind erosion modelling, and is estimated here from vegetation characteristics. We use the parameterizations of ground surface characteristics established by *Pierre et al.* (2015; equation (8)) to estimate z_0 for spontaneous herbaceous, and by *Pierre et al.* (2018; equations (2) to (6)) to estimate E and z_0 for millet. These parametrizations account for the distinct geometry of millet and herbaceous as they have been empirically defined for each of these two cover types. They depend on vegetation mass or vegetation cover, and they distinguish between standing and prostrate (i.e. litter) vegetation (see Appendix C).

2.3.2 Vegetation models

The STEP model (*Mougin et al.,* 1995) was developed to simulate the growth of seasonal Sahelian herbaceous vegetation, while the SarraH model (*Baron et al.,* 2005) simulates crop growth for millet. Both vegetation models have been extensively tested for several Sahelian study sites (e.g. *Tracol et al.*, 2006; *Pierre et al.,* 2011 for STEP; and *Kouressy et al.,* 2008; *Marteau et al.,* 2011 for SarraH). They run on a daily time step, using meteorological data and soil texture information as inputs, and providing vegetation mass and Leaf Area Index (LAI) as main outputs. The SarraH model further provides grain yields as well as separate stalk and leaf mass. Among dry vegetation, standing straws inhibit more wind erosion than prostrate litter due to their larger effectiveness at reducing wind momentum near the surface (e.g. *Pi et al.,* 2020). Thus we need information on both dry vegetation types. STEP already had a dry season submodel to simulate dry vegetation during the dry season. SarraH has been added a dry season submodel to simulate crop residue dynamics after harvest (*Pierre et al.,* 2015; see also Appendix B). According to these dry season submodels, livestock ingests part of dry leaves, and tramples dry stems

and leaves, while abiotic factors also induce vegetation degradation. Grazing pressure was assumed to be spatially homogenous over all land uses.

STEP and SarraH models require parameters related to agro-pastoral practices. Namely, these parameters are:

(i) for STEP: soil fertility and grazing pressure,

(ii) for SarraH: cultivar, intensity of the use of manure, sowing date, sowing density, proportion of collected residues at harvest, proportion of residues laid down at harvest, grazing pressure (after harvest) and date of field clearing (date at which all remaining standing residues are laid down on the soil).

In SarraH, grazing pressure is only applied to dry vegetation, in line with the exclusion of livestock from Sahelian cropped fields during the rainy season. In STEP, a light grazing effect on green vegetation is implicitly accounted for in the growth parameters, while grazing pressure is applied in the dry season. Soil fertility is taken into account through a productivity coefficient. Here, we adjusted the productivity coefficient to attain target herbaceous and millet production levels for each set of practices under the scenarios (see *2.3.4*).

2.3.3 Meteorological data

In order to separate effects of climate change from land management practices, the simulations were run for each land use and associated set of management practices using the same meteorological 12-year series. As in *Pierre et al.* (2018), we used meteorological data (wind speed, air temperature, relative humidity, and precipitation) monitored in Banizoumbou since 2006 at 6.5 m height with 5-min resolution (*Marticorena et al.,* 2017), but over a longer period (2006-2017). Temporal coverage of meteorological measurements was very good with less than 3% of missing wind and rainfall data. Solar radiation data were re-analyses of the European Center for Medium-Range Weather Forecast (ERA-Interim; *Dee et al.,* 2011). Meteorological data were converted to daily values for vegetation modelling, whereas 5-minutes wind and rainfall data were used for wind erosion modelling. Horizontal aeolian flux was then summed to get daily, seasonal and annual values for the analysis. Following *Bergametti et al.* (2016; pers. comm.), simulated wind erosion was assumed to be nil for rains larger than 0.4 mm in 4 hours, from rain start to 12 h after the end of the rain event (the end of the event being defined as soon as there is no rain during 4 hours).

Meteorological conditions at the study site exhibit a large interannual variability (*Table 1*). The mean annual rainfall over the used time-series is 505 mm with a standard deviation of 144 mm. The proportion of high wind speeds (greater than 7 $m.s^{-1}$, at 5-minutes resolution, 6.5m height, corresponding to wind erosion threshold for the bare soil at the study site, see *Abdourhamane Toure et al.,* 2011) was also highly variable through years with a mean of 1.35 % and a standard deviation of 0.63%.

	2006	2007	2008	2009	2010	2011	2012	2013	2014	2015	2016	2017	mean	std	std/mean
Rainfall (mm)	533	471	698	307	371	349	807	504	432	584	548	450	505	144	0.28
Prop wind >7 m.s^{-1} (%)	*2.24*	*2.29*	*2.08*	*1.41*	*1.68*	*1.35*	*1.52*	*0.84*	*0.68*	*0.98*	*0.54*	*0.59*	1.35	0.63	0.47

Table 1: Interannual variability of meteorological conditions over the 12-year period

2.3.4 Sets of simulations

Detailed information about simulation names and parameters are reported in *Table 2*. Note that given land uses (e.g. manured fields) exhibit different associated land management practices among scenarios.

In the *Low Density* scenario, the soil fertility of savanna - in the grassland vegetation model (STEP), used in the 'Sav1950s' simulation - was set to produce an annual maximum mass of green vegetation of about 180 g.m^{-2} (237 g.m^{-2} for the sum of standing green and dry vegetation) on average for the 12-year meteorological data used, to be in agreement with observations (see Table 28 in *Hiernaux and Ayantunde*, 2004).

Simulation name	Land use	Vegetation model	Parameters	Simulated mass (mean of annual max)
Sav1950s	Savanna	STEP	*Soil fertility: 3.4*	Green: 182 g.m^{-2}
			Grazing Pressure: 0 TLU.km^{-2}	Tot: 237 g.m^{-2}
Fal1990s	Fallows	STEP	*Soil fertility: 2.9*	Green: 142 g.m^{-2}
			Grazing Pressure: 8 TLU.km^{-2}	Tot: 156 g.m^{-2}
FieldBush1990s	Unmanured fields	SarraH	*Manure: none (NF)*	Grains: 104 g.m^{-2}
			Sowing density: 6000 plants.ha^{-1}	Stalks:152 g.m^{-2}
			Residues collecting: 10%	Leaves: 56 g.m^{-2}
			Residues laid down: 0%	
			Grazing pressure: 8 TLU.km^{-2}	
FieldHome1990s	Manured fields	SarraH	*Manure: slight (mF)*	Grains: 124 g.m^{-2}
			Sowing density: 10 000 plants.ha^{-1}	Stalks: 241 g.m^{-2}
			Residues collecting: 10%	Leaves: 56 g.m^{-2}
			Residues laid down: 0%	
			Grazing pressure: 8 TLU.km^{-2}	
FieldExt2030s	Unmanured fields	SarraH	*Manure: none (NF)*	Grains: 102 g.m^{-2}
			Sowing density: 4 000 plants.ha^{-1}	Stalks: 134 g.m^{-2}
			Residues collecting: 75%	Leaves: 54 g.m^{-2}
			Residues laid down: 0%	
			Grazing pressure: 12 TLU.km^{-2}	

FieldInt2030s	Manured fields	SarraH	*Manure: high (F)*	Grains: 128 g.m^{-2}
			Sowing density: 12 000 plants.ha^{-1}	Stalks: 345 g.m^{-2}
			Residues collecting: 75%	Leaves: 61 g.m^{-2}
			Residues laid down: 10%	
			Grazing pressure: 20 TLU.km^{-2}	

Table 2: Simulation names and models parameters

In the *High Density* scenario, the soil fertility in fallows (simulation 'Fal1990s' with STEP model) was lower than in savannas of the *Low Density* scenario, due to nutrient depletion induced by shifting cultivation (*Turner and Hiernaux,* 2015). It was adjusted to produce an annual maximum mass of green vegetation of about 140 g.m^{-2} (150 g.m^{-2} for the sum of standing green and dry vegetation) on average over the 12-year period, to be in agreement with observations (Table 28 in *Hiernaux and Ayantunde*, 2004). Similarly, the soil fertility in millet fields was set (in the crop model SarraH) to simulate a total aboveground mass of about 312 g.m^{-2} for unmanured fields (simulation 'FieldBush1990s') and 421 g.m^{-2} for manured fields (simulation 'FieldHome1990s'), close to the values observed by *Hiernaux and Ayantunde* (2004; Table 28). The simulated vegetation amounts for stalks (152 and 241 g.m^{-2}) and for leaves (56 g.m^{-2} in both cases) were also in fair agreement with observations. Simulated grain amounts (104 and 124 g.m^{-2}) were large and likely overestimated. However, grains are filled during the late rainy season, when vegetation cover already prevents wind erosion, and they are collected at harvest, and so do not play a role for soil protection during the dry season. Therefore, the uncertainty in simulated grain amounts was not problematic for our study. For the *High density* scenario, livestock density was assumed to be balanced with forage availability over the study site (see Appendix A for the estimate of the grazing pressure).

Both *Very high density* scenarios are prospective and thus do not compare with observations. They assume cropland expansion over all the arable land in the simulation area. There was no manure effect for the croplands of the *Extensive* scenario (simulation 'FieldExt2030s' with SarraH model) and a full manure and fertilizer effect for the croplands of the *Intensive* scenario (simulation 'FieldInt2030s' with SarraH model). Accordingly, millet sowing density was high for *Intensive* and low for *Extensive*, while grazing pressure increased slightly in *Extensive* and significantly in *Intensive*, compared to the *High density* scenario.

For all scenarios including croplands (*High density*, *Very high density, Extensive* and *Very high density, Intensive*), the cultivar was millet Haini Kirey, sown on June 7th and fields were cleared on March 1st. These practices were set up in agreement with previous work (*Pierre et al.,* 2018) as they were not prone to change under the socio-environmental conditions defining the scenarios.

3. Results

3.1 Per land use:

Wind erosion depends on the occurrence of strong winds combined with a low soil protection by vegetation. Thus, we must scrutinize *(i)* the seasonality of vegetation to understand *(ii)* the seasonality of horizontal sediment flux and ultimately *(iii)* its annual amounts. Vegetation mass is of particular interest, as it is a relevant variable to estimate the drag partition of the wind due to vegetation (see *2.3.1*).

3.1.1 Vegetation mass seasonality

For the same meteorological conditions, differences were large between millet and herbaceous mass (see *Table 3* for pluriannual amounts, and *Figure 4* where 2010 illustrates the seasonality of vegetation growth). At the beginning of the rainy season, herbaceous growth was faster than millet growth, while the maximum standing mass was much larger for millet than for herbaceous (*Figure 4a*). As described below, differences are also noticeable between simulations for each vegetation type.

Herbaceous:

'Sav1950s' and 'Fal1990s' simulations exhibited the same dynamics (e.g. onset of vegetation growth in early June and maximum in late September, see *Figure 4b*) but lower green vegetation maximum amounts for 'Fal1990s' (140 $g.m^{-2}$ in 2010, 142+/-25 $g.m^{-2}$ pluriannual mean) than for 'Sav1950s' (174 $g.m^{-2}$ in 2010, 182+/-32 $g.m^{-2}$ pluriannual mean) due to a lower soil fertility. Similarly, standing straws reached larger maximum amounts for 'Sav1950s' (144 $g.m^{-2}$ end of October in 2010; 138+/-16 $g.m^{-2}$ pluriannual mean) than for 'Fal1990s' (87 $g.m^{-2}$ in 2010; 83+/-14 $g.m^{-2}$ pluriannual mean) because of the difference in green vegetation amounts and because the grazing pressure increased from 0 for 'Sav1950s' to 8 $TLU.km^{-2}$ for 'Fal1990s'. This grazing pressure also induced a faster decrease of standing straws amounts for 'Fal1990s' than for 'Sav1950s'. As trampling transforms straws into litter, litter amounts became slightly larger for 'Fal1990s' during the dry season (from December to April; maximum of 31 $g.m^{-2}$ in 2010; 30+/-4 $g.m^{-2}$ as pluriannual mean), before reaching lower values than for 'Sav1950s' (maximum of 24 $g.m^{-2}$ in 2010; 25+/-3 $g.m^{-2}$ as pluriannual mean) at the end of the dry season. Altogether, annual minimum amounts of total vegetation were thus lower for 'Fal1990s' (24 $g.m^{-2}$ in 2010 -, 20+/-6 $g.m^{-2}$ pluriannual mean) than for 'Sav1950s' (77 $g.m^{-2}$ in 2010, 77+/-10 $g.m^{-2}$ pluriannual mean). This minimum value was usually reached by the end of June (e.g. June 26th in 2010).

Millet:

A larger soil fertility and larger plant density yielded a larger green vegetation amount for 'FieldHome1990s' compared to 'FieldBush1990s' over the whole rainy season, along with a faster

increase in green vegetation mass at growth onset (*Figure 4c*). Maximum green vegetation in 2010 was 483 g.m^{-2} for 'FieldHome1990s' (409+/-108 g.m^{-2} pluriannual mean) and 377 g.m^{-2} for 'FieldBush1990s' (307+/-113 g.m^{-2} pluriannual mean). The same observation applied between 'FieldHome1990s' and 'FieldInt2030s', with a larger soil fertility and plant density for the latter, yielding the largest maximum green vegetation amount (608 g.m^{-2} in 2010; 519+/-123 g.m^{-2} pluriannual mean). Maximum green vegetation amounts were similar between 'FieldBush1990s' and 'FieldExt2030s' (351 g.m^{-2}; 286+/-110 g.m^{-2} pluriannual mean), the only difference stemming from green vegetation having a slightly larger plant density for 'FieldBush1990s' (6000 plants.ha^{-1}) than for 'FieldExt2030s' (4000 plants.ha^{-1}). These observations held true for every year and for each part of the plant (grains, stems, leaves; not shown).

Differences in crop residue management induced contrasting behaviors for dry vegetation (standing straws, that include standing dry stems and leaves; and litter, that include flattened dry stems and leaves) compared to green vegetation. 'FieldHome1990s' yielded the largest standing straw mass (maximum of 291 g.m^{-2} in 2010; 243+/-81 g.m^{-2} pluriannual mean), followed by 'FieldBush1990s' (215 g.m^{-2} in 2010; 173 +/- 76 g.m^{-2} pluriannual mean). Although the difference in green vegetation amounts was slight between 'FieldBush1990s' and 'FieldExt2030s', it became larger for standing straws because of the larger proportion of crop residues collected at harvest for 'FieldExt2030s' (54 g.m^{-2} in 2010; 43+/-20 g.m^{-2} pluriannual mean) compared to 'FieldBush1990s'. Similarly, the large proportion of crop residues collected at harvest for 'FieldInt2030s' (that occurred usually at the beginning of October, e.g. October 9th in 2010) yielded a low maximum amount of standing straws after harvest (65 g.m^{-2} in 2010; 55 +/-16 g.m^{-2} pluriannual mean), although this simulation produced the largest green vegetation amounts. It was also similar to 'FieldExt2030s', which produced the lowest green vegetation amounts. 'FieldInt2030s' was the only simulation in which some of the residues were laid down as litter at harvest.

For all millet simulations, field clearing on March 1st induced a sharp increase in litter mass. From then on, as for the mass of standing straws, litter mass was the largest for 'FieldHome1990s' (maximum of 142 g.m^{-2} in 2010; 120+/-49 g.m^{-2} pluriannual mean), intermediate for 'FieldBush1990s' (98 g.m^{-2} in 2010; 81+/-43 g.m^{-2} pluriannual mean), and the lowest for 'FieldInt2030s' (44 g.m^{-2} in 2010; 37+/-11 g.m^{-2} pluriannual mean) and 'FieldExt2030s' (18 g.m^{-2} in 2010; 15+/-8 g.m^{-2} pluriannual mean). As they considered the same grazing pressure, 'FieldHome1990s' and 'FieldBush1990s' exhibited the same rate of decrease of dry vegetation amounts. 'FieldInt2030s' decreased faster than 'FieldExt2030s' because of a larger grazing pressure; their litter masses were very small (e.g. about 2 g.m^{-2} at the beginning of June 2010, versus 15 g.m^{-2} for 'FieldBush1990s' and 23 g.m^{-2} for 'FieldHome1990s').

Although maximum mass of standing straws was of similar magnitude between some herbaceous and millet simulations ('FieldBush1990s' and 'Sav1950s'; 'FieldInt2030s' and 'Fal1990s'), this did not hold true during the dry season due to contrasting rates of decrease of dry vegetation. Altogether, annual minimum mass of total vegetation reached much lower values for millet than for grass, ranging between

0.6+/-0.2 g.m^{-2} for 'FieldInt2030s' (0.6 g.m^{-2} in 2010) to 12+/-5 g.m^{-2} for 'FieldHome2030s' (13.5 g.m^{-2} in 2010), also usually reached at the end of June (June 27th in 2010, July 24th for 'FieldBush1990s').

Simulation	Green max	Straws max	Litter max	Total min
Sav1950s	182+/-32	138+/-16	25+/-3	77+/-10
Fal1990s	142+/-25	83+/-14	30+/-4	20+/-6
FieldHome1990s	409+/-108	243+/-81	120+/-49	12+/-5
FieldBush1990s	307+/-113	173 +/- 76	81+/-43	7+/-4
FieldExt2030s	286+/-110	43+/-20	15+/-8	1+/-0.7
FieldInt2030s	519+/-123	55 +/-16	37+/-11	0.6+/-0.2

Table 3: Pluriannual mean and standard deviation of annual maximum and minimum vegetation mass (in g.m^{-2}) for the 6 simulations

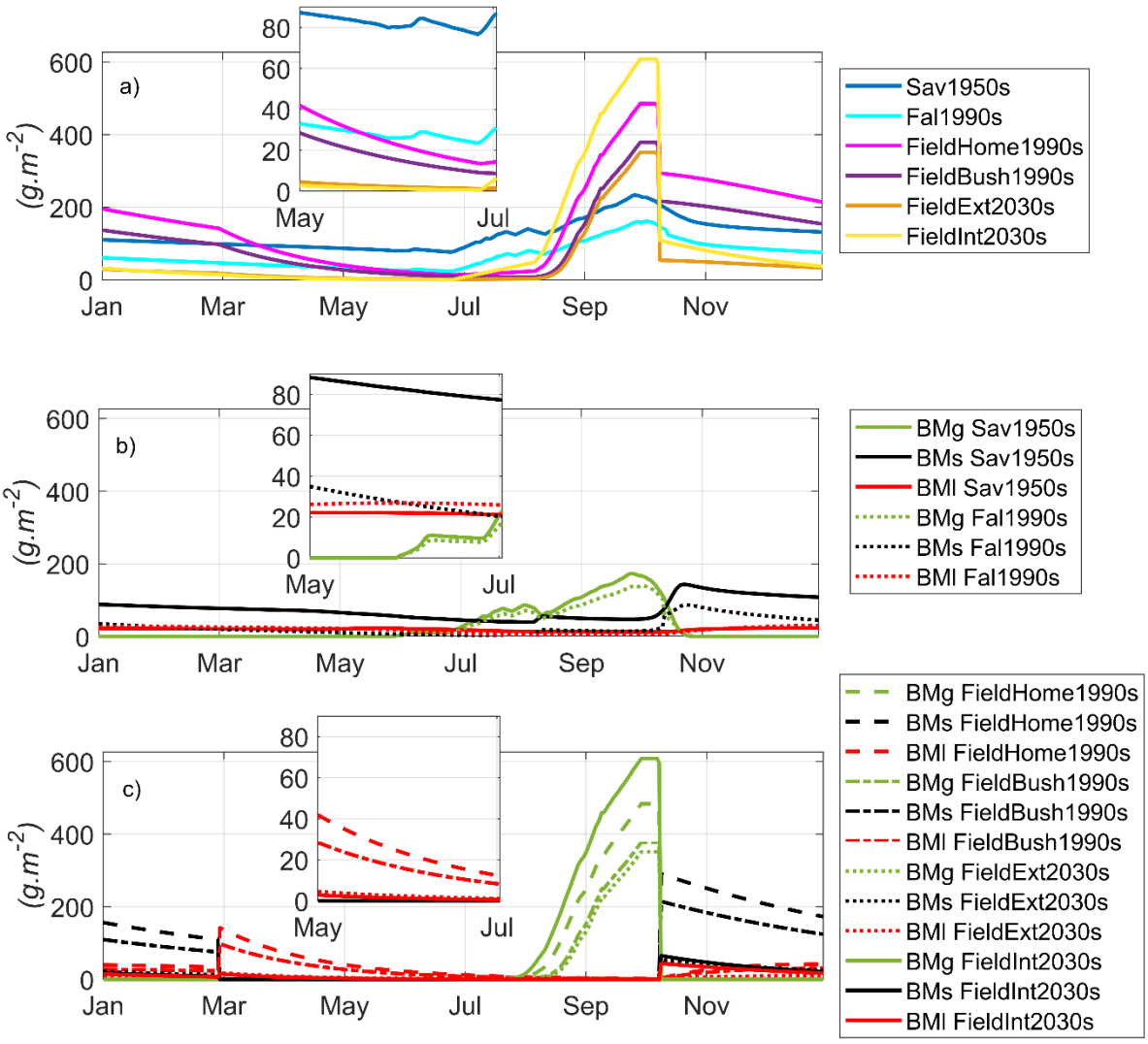

Fig. 4 *Vegetation amounts in 2010 for a) total vegetation for the 6 simulations, b) green vegetation (BMg), standing straws (BMs) and litter (BMl) for the 2 herbaceous simulations, and c) the 4 millet simulations*

3.1.2 Horizontal sediment flux seasonality

Table 4 presents the pluriannual means of monthly horizontal sediment flux and *Figure 5* illustrates its seasonality for year 2010, with an additional case of bare soil for comparison, enabling to assess the impact of meteorological conditions only, although this latter case is not realistic in terms of land management. In all cases, horizontal sediment flux was nil to negligible from August to January, suggesting that meteorological conditions yielded no wind erosion during that period. Both prospective simulations led to non-negligible amounts from January to March, yet lower than for bare soil, indicating that the dry vegetation cover reduced wind erosion during that time, even for low amounts of vegetation mass. In spring (April to July), monthly amounts of horizontal sediment flux were nil to negligible for herbaceous cover, intermediate for the 1990s croplands and large for 'future' croplands. During (late) spring, horizontal sediment flux for bare soil was similar to that for 'FieldExt2030s' and 'FieldInt2030s' ('FieldBush1990s'), as vegetation cover had almost disappeared at that time in these simulations. Altogether, the horizontal sediment flux was thus the largest for croplands, especially in May (46+/-102 kg.m^{-1} for 'FieldHome1990s' to 196+/-162 kg.m^{-1} for 'FieldInt2030s' kg.m^{-1}), June (111+/-107 kg.m^{-1} for 'FieldHome1990s' to 238+/-144 kg.m^{-1} for 'FieldExt2030s' kg.m^{-1}) and July (59+/-87 and 59+/-78 kg.m^{-1} for 'FieldHome1990s' and 'FieldInt2030s' to 104+/-88 kg.m^{-1} for 'FieldExt2030s' kg.m^{-1}). Monthly horizontal sediment fluxes were constantly larger for 'FieldBush1990s' than for 'FieldHome1990s', mostly from May to July, as threshold friction velocity (u_{*t}) was always larger for 'FieldHome1990s' than for 'FieldBush1990s' due to larger vegetation amounts. In 2010, this threshold reached a minimum value of 47.9 cm.s^{-1} for 'FieldBush1990s' on July 24th and 58.0 cm.s^{-1} for 'FieldHome1990s' on June 27th (not shown).

The difference in horizontal sediment flux between 'FieldExt2030s' and 'FieldInt2030s' was slight and resulted from seasonal differences in vegetation cover. Crop residue management yielded close amounts of litter for both simulations, yet with slightly larger amounts for 'FieldExt2030s' than for 'FieldInt2030s' at the end of the dry season due to a larger grazing pressure for 'FieldInt2030s'. Thus, the threshold friction velocity was larger for 'FieldExt2030s' than for 'FieldInt2030s' at the end of the dry season and became lower at the beginning of the rainy season (not shown). For example, in 2010 u_{*t} reaches a minimum value of 25.2 cm.s^{-1} for 'FieldInt2030s' and 29.0 cm.s^{-1} for 'FieldExt2030s' on June 27th, before increasing to 38.6 cm.s^{-1} for 'FieldInt2030s' but only to 29.7 cm.s^{-1} for 'FieldExt2030s' on July 1st because of the larger soil fertility and sowing density in 'FieldInt2030s'. This fast increase for 'FieldInt2030s' after vegetation germination prevented wind erosion earlier in the year than for

'FieldExt2030s'. Altogether, the horizontal sediment flux was thus larger for 'FieldInt2030s' at the end of the dry season (May-June) and larger for 'FieldExt2030s' during the beginning of the rainy season (end of June to beginning of August).

Simulation	Jan	Feb	Mar	Apr	May	Jun	Jul	Aug	Sep	Oct	Nov	Dec
Sav1950s	0	0	0	0	0	0	0	0	0	0	0	0
Fal1990s	0	0	0	0	0	12+/-17	8+/-16	0	0	0	0	0
FieldHome1990s	0	0	0	0	46+/-102	111+/-107	59+/-87	1+/-2	0	0	0	0
FieldBush1990s	1+/-5	0	0	7+/-14	89+/-161	159+/-136	82+/-101	3+/-5	0	0	0	0
FieldExt2030s	19+/-55	12+/-28	21+/-39	72+/-93	178+/-171	238+/-144	104+/-88	6+/-9	0	0	0	1+/-2
FieldInt2030s	3+/-9	1+/-3	6+/-10	64+/-68	196+/-162	237+/-147	59+/-78	1+/-2	0	0	0	0
Bare soil	*64+/-91*	*64+/-59*	*111+/-68*	*129+/-93*	*234+/-152*	*246+/-132*	*108+/-77*	*22+/-10*	*22+/-12*	*11+/-12*	*9+/-11*	*18+/-16*

Table 4: Pluriannual mean and standard deviation of monthly horizontal sediment flux (in kg.m^{-1}) for the 6 simulations, and a bare soil

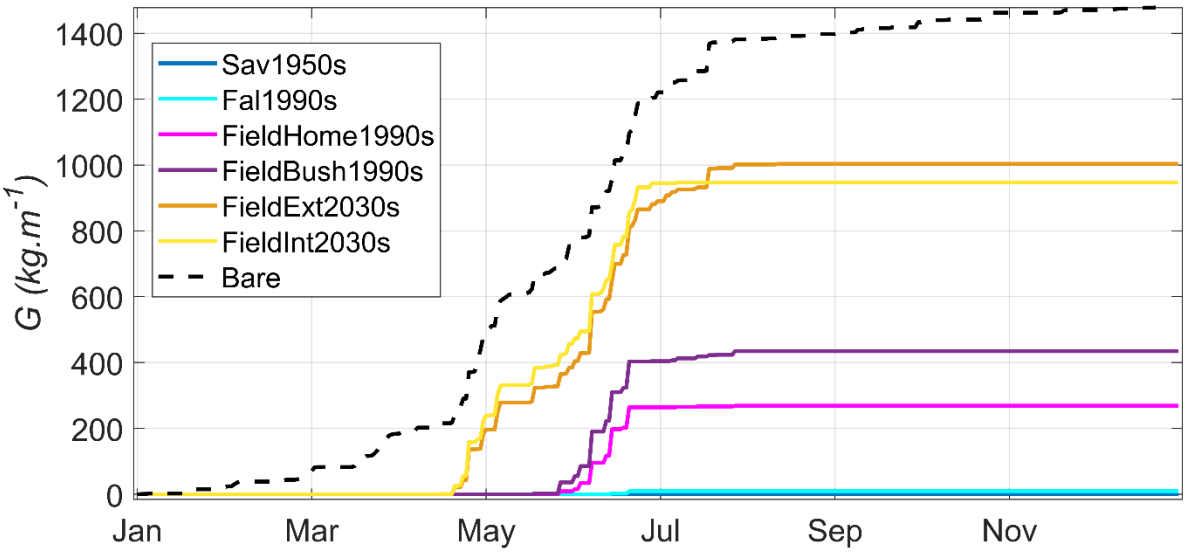

Fig. 5 *Cumulated daily horizontal sediment flux G for the 6 simulations and a bare soil in 2010.*

3.1.3 Mean annual horizontal sediment flux

The mass of total horizontal sediment fluxes and its annual mean were computed for each simulation (i.e. for each land unit) and for a bare soil over the 12-year period. As observed in the previous subsections, the vegetation cover of 'Sav1950s' was always large enough to prevent wind erosion, notably because of a large soil fertility and no grazing pressure. The decrease in soil fertility and the intermediate grazing pressure in 'Fal1990s' compared to 'Sav1950s' yielded a low horizontal sediment flux of 20+/-28 kg.m^{-1} per year on average.

In agreement with the seasonality discussed above, 'FieldHome1990s' yielded the lowest annual horizontal sediment flux among the four cultivated cases (217+/-263 $kg.m^{-1}.yr^{-1}$) due to a large soil fertility and a low rate of residue collection and thus large vegetation amounts protecting the soil from wind during the rainy season and the dry season. Conversely, 'FieldExt2030s' yielded the largest horizontal sediment flux (649+/-515 $kg.m^{-1}.yr^{-1}$), in response to residue collection, yet about 1.6 times lower than a bare soil (1037+/-533 $kg.m^{-1}.yr^{-1}$). It was closely followed by 'FieldInt2030s' (565+/-396 $kg.m^{-1}.yr^{-1}$), which produced larger green vegetation amounts than 'FieldExt2030s' thanks to manure and fertilizers, but had some residues laid down at harvest (in addition to residue collection) and a larger grazing pressure on dry vegetation from then on. 'FieldBush1990s' yielded intermediate values of horizontal sediment flux (341+/-363 $kg.m^{-1}.yr^{-1}$), with a low soil fertility but also a very low proportion of residue being collected. Standard deviations over the 12-year series were large, yet the relative order of annual sediment fluxes remains every year, from 'FieldExt2030s' yielding the largest values to 'Sav1950s' yielding the lowest ones.

3.2 Landscape scale responses

3.2.1 Mean annual horizontal sediment flux

Mean annual horizontal sediment flux for scenarios are reported in *Figure 6*, as weighted combinations of the simulations over the whole landscape according to the corresponding land use proportions, including the plateaus (see *Figure 2*). Under the *Low density* scenario, annual horizontal sediment flux remained zero across the landscape. For the *High density* (1990s) scenario, the combination of fallows, unmanured and manured fields, and plateaus, yielded an average horizontal sediment flux of 176 $kg.m^{-1}.yr^{-1}$. The weighing slightly reduced the values for both future scenarios (*Very high density, Extensive:* 520 $kg.m^{-1}.yr^{-1}$ and *Very high density, Intensive*: 452 $kg.m^{-1}.yr^{-1}$) compared to single land uses, as their estimates included 20% of the landscape covered by plateaus that are not prone to wind erosion. Similarly, bare soil would induced a horizontal sediment flux of 830 $kg.m^{-1}.yr^{-1}$ over the landscape, with no wind erosion over the plateaus.

Thus, the fact that landscapes are composed of several land uses had a noticeable influence on the final results among scenarios. As an example, the unmanured fields of the *High density* scenario ('FieldBush1990s') produced a mean annual horizontal sediment flux of 341 $kg.m^{-1}.yr^{-1}$. Yet, under the *High density* scenario, unmanured fields constitute only 45% of the landscape (and fallows, manured fields, and plateaus respectively 20%, 8%, and 20% of the landscape), yielding a landscape scale horizontal sediment flux (per unit area) much lower than for unmanured fields only.

As for the land use estimates, the landscape scale values exhibited large standard deviations over the 12-year time series (not shown), yet the relative order of annual sediment fluxes remained consistent

every year, from *Very high density, Extensive* yielding the largest amounts to *Low density* yielding the lowest.

Altogether, these mean annual horizontal sediment fluxes differed by approximately a factor 2.5 to 3 between *High density* and *Very high density*, while *Low density* yields no wind erosion. Thus, both future scenarios suggest a significant increase of wind erosion compared to historical and recent situations (under current meteorological conditions). However, both yielded a lower horizontal sediment flux than bare soil (1.6 times lower for *Extensive* and 1.8 times lower for *Intensive*). The *Extensive* scenario yielded slightly larger values of horizontal sediment flux than the *Intensive* one, related to lower green vegetation amounts in *Extensive*, which is not totally counterbalanced by the lower use of crop residues in *Extensive* compared to *Intensive*.

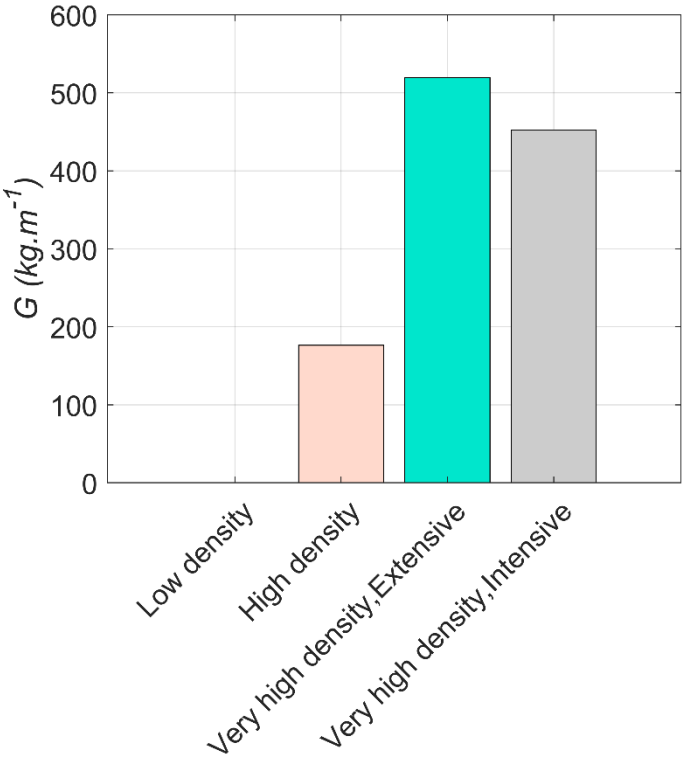

Fig. 6 *Annual mean horizontal sediment flux over the 12-year period for all scenarios*

3.2.2 Wind erosion frequencies and large events

For present-day meteorological conditions, the frequency of days with wind erosion ranged from 0 for *Low Density* to 15.5% for *Very High Density, Extensive* (and 44.1% for bare soil), with lower values of 11.9% for *Very High Density, Intensive* and 5.9% for *High Density* (*Table 5*). Thus, land use and land management had an impact on both total amount and frequency of horizontal sediment flux. In addition, any land use and land management simulated here largely reduced the occurrence of wind erosion compared to a bare soil, especially for small events.

Most of the erosive days occurred in May, June and July, with 70% (*Very high density, Extensive*) to 77% (*Very high density, Intensive*) and 88% (*High density*) of events occurring over this period (not shown). Large events, with horizontal sediment flux larger than 50 kg.m^{-1} per day, also concentrate between mid-May and early July. They sum up to 19%, 19%, and 21% of the total sediment flux of the 12-year period for *High density, Very high density, Extensive* and *Very high density, Intensive*, respectively, although they represented only about 3% of the erosive days. These figures emphasize the large seasonality of wind erosion, which persisted with a mosaic of land uses over the simulated landscape.

In addition, the differences in total amounts of horizontal sediment flux between the *High Density* and the *Very High Density* scenarios were related to significant differences in the frequencies at which the landscape was prone to wind erosion, for all kind of events. Between *Extensive* and *Intensive*, the differences were mostly due to days with horizontal sediment flux lower than 20 kg.m^{-1}, as the frequencies of days with larger events were similar.

Large aeolian sediment transport events can abrade plants, especially if they occur during the beginning of plant growth (*Sterk*, 2003). Here, maximum daily horizontal sediment flux was about 100 kg.m^{-1} (102 kg.m^{-1} on May 13th 2008 and 108 kg.m^{-1} on June 29th 2008 for *Very high density, Intensive*; 100 kg.m^{-1} on June 9th 2010 for *Very high density, Extensive*; versus 111 kg.m^{-1} on May 13th 2008 for a bare soil), occurring in croplands at the end of the dry season. Maximum daily horizontal sediment flux for *High density* was 71 kg.m^{-1} (on July 4th 2008). Given that most wind erosion events lasted less than 1 hour (not shown), these figures compare with the ones from *Michels et al.* (1995), who noticed a significant abrasion effect on millet seedlings after horizontal sediment flux of about 37 kg.m^{-1} over 15 minutes.

Scenario	Freq. of days with wind erosion > 0 kg.m^{-1} (%)	Freq. of days with wind erosion > 20 kg.m^{-1} (%)	Freq. of days with wind erosion > 50 kg.m^{-1} (%)
Low density (1950s)	0	0	0
High density (1990s)	5.9	0.8	0.2
Very high density, Extensive (2030s)	15.5	2.2	0.4
Very high density, Intensive (2030s)	11.9	2.2	0.4
Bare soil	44.1	4	0.6

Table 5: Frequency of days with wind erosion larger than 0, 20 or 50 kg.m^{-1} for each scenario and the bare soil over the 12-year period

3.2.3 Interannual variability of horizontal sediment flux

The large interannual variability of meteorological conditions raises the question of the extent to which cropping practices may prevent wind erosion, compared to the variability of wind erosion due to meteorological conditions. For each scenario, annual horizontal sediment flux exhibited large interannual variability, about the same order as its pluriannual mean (see *Table D1* in Appendix D). Thus, for the same practices, meteorological conditions induced large variability in the annual horizontal sediment flux (of about 70% to 105%, depending on the scenario).

Similarly, each year, the variability of the horizontal sediment flux among scenarios was about the same order as its mean over the four scenarios (*Table D2*; this does not include the bare soil case). Thus, for the same meteorological conditions, land management induced large variability in the horizontal sediment flux (of about 80 to 110%). Altogether, the variability of annual horizontal sediment flux due to land management was of the same order as that due to meteorological conditions. While such observations were made on benchmark simulations (*Pierre et al.,* 2018), these results show that realistic sets of practices have as large an influence as the largest theoretical range of practices on the variability of annual horizontal sediment flux.

More specifically, the results show that:

1) Management promoting wind erosion tended to reduce annual wind erosion relative variability related to meteorological conditions (see e.g. the low values of the coefficients of variation over years of 0.70 and 0.79 for *Very high density, Extensive* and *Intensive* in *Table D1*, with both scenarios associated with the largest horizontal sediment fluxes; the latter decreased to 51% for the case of a bare soil).

2) Conversely, the relative variability of annual horizontal sediment fluxes between scenarios (i.e. due to management) tended to be the lowest when high winds were the most frequent. There was a significant ($p<0.05$) anticorrelation ($R=-0.65$) between the annual frequencies of high wind events and the relative variability of annual horizontal sediment fluxes in *Table D2* ($n=12$).

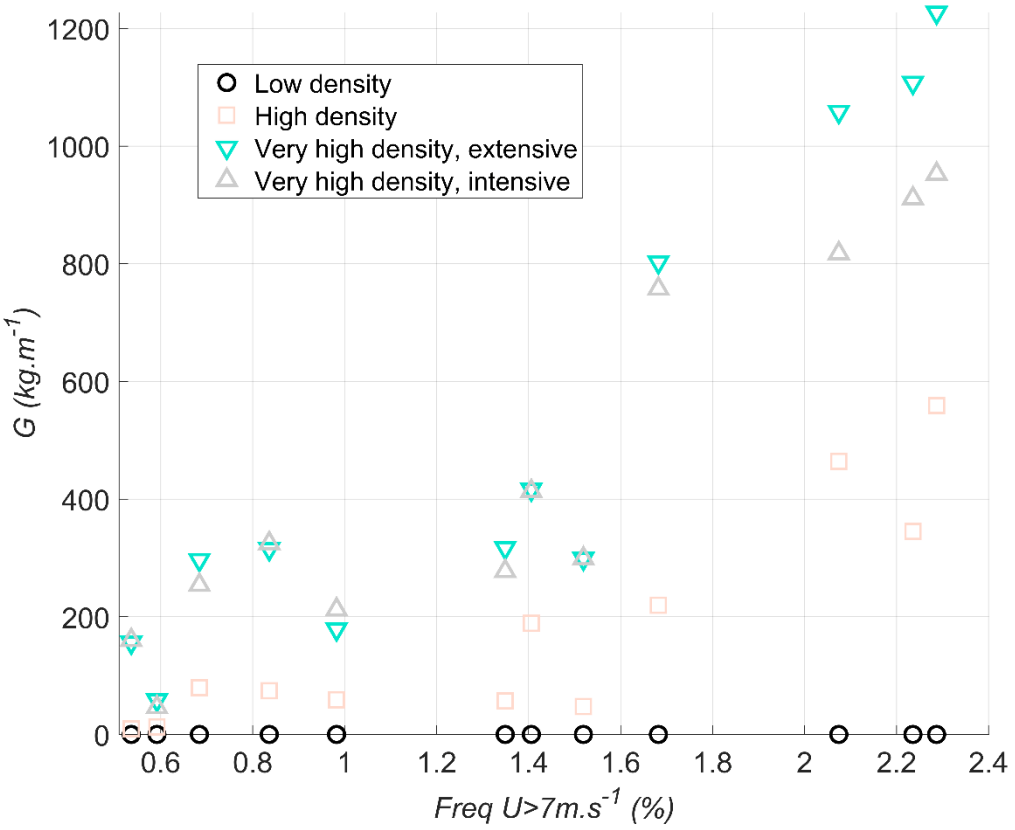

Fig. 7 *Annual horizontal sediment flux versus frequency of large winds over the 12-year period for all scenarios*

Additionally, there was a correlation of about 0.9 (n=12, p-value<0.0005) between the annual horizontal sediment flux and the frequency of winds higher than 7 ms^{-1} for all landscapes (*Figure 7*). This correlation was larger for both *Very high density* scenarios (R=0.92 for Extensive, 0.93 for Intensive) than for the *High density* situation (R=0.87). This trend is driven by cropped land uses, while fallows in the *High density* landscape yielded a correlation lower than 0.3 (not shown). Indeed, for cropped surfaces, the low vegetation cover during the erosive period of the year allowed wind erosion to mainly depend on wind conditions.

4. Discussion

The steady increase in rural population density since the 1950s induced a widespread cropland expansion throughout the Sahel (*van Vliet et al.,* 2013; *Tappan et al.,* 2016). As lands are becoming increasingly cultivated, fields are less often fallowed and generally with no chemical fertilizer applied (though manure can be applied in fields located close to villages or pastoralist camps) and soil fertility tends to decline (*Turner and Hiernaux,* 2015). Meanwhile, crop residues are increasingly collected (although not necessarily exported from the village territory), which has a large impact on wind erosion

as the surface becomes less protected from wind. Both phenomena, decrease in soil fertility and increase in crop residues collection, have been observed and reported in the literature, including in southwestern Niger (*Schlecht et al.,* 2001; *Akponikpè et al.,* 2014).

Our simulations show that a consequence of these changes is an increasing horizontal airborne sediment flux, from nil flux with 1950s land management (*Low density*) to intermediate values with 1990s land management (*High density*) and large values with potential land management in 2030s (*Very high density*). Also, as weighted mean of land uses composing each landscape, available forage (maximum annual amounts of grass and millet leaves) decreases from 189 $g.m^{-2}$ (*Low density*) to 72 $g.m^{-2}$ (*High density*) and to 49 $g.m^{-2}$ (*Very high density, Intensive*) or 43 $g.m^{-2}$ (*Very high density, Extensive*). Thus, the disappearing of fallows and rangelands in the prospective scenarios led to a decrease in forage availability and an increase in horizontal sediment flux compared to historical and recent situations.

The horizontal sediment flux was only slightly lower for the *Intensive* prospective scenario (based on a tight combination of cropping and livestock farming) than for the *Extensive* one (with increased use of current practices and soil depletion), although intensification could enable larger amounts of grain and forage production. This difference in vegetation amounts was due to practices enhancing green vegetation growth in *Intensive* (manuring and sowing density), allowing a higher collection of crop residues while keeping horizontal sediment flux of the same magnitude as in the *Extensive* scenario. Compared to the *Extensive* scenario, *Intensive* provides sensibly higher grain yields, slightly higher mass of millet leaves, and much larger stalks mass. The latter constitutes a resource as they can be sold, e.g. as building material (yet they are not palatable for livestock). Their annual maximum amounts ranged from 0 for *Low density* (no millet fields) to 88 $g.m^{-2}$ for *High density*, 107 $g.m^{-2}$ for *Very high density, Extensive* and 276 $g.m^{-2}$ for *Very high density, Intensive*.

Thus, although the *Intensive* prospective scenario yielded larger vegetation production, it resulted in horizontal sediment fluxes of similar magnitude to the *Extensive* scenario. Such large horizontal sediment fluxes could deplete soil fertility and thus increasingly require the use of fertilizers, reducing the long-term sustainability of such a scenario. This result could help designing future land management policies to assess wind erosion risk along with other ecological issues like forage production and soil nutrients depletion.

Altogether, the simulated values were in good agreement with the few existing observations (*Table 6*), in terms of vegetation amounts as well as horizontal sediment flux, for both vegetation types.

	Millet	Herbaceous
Annual maximum mass of total vegetation ($g.m^{-2}$)	300-500 *Marteau et al.,* 2011 (Niamey area, 2004-2009) 200-300 *Rockström & de Rouw,* 1997 (Banizoumbou, 1994-1996)	40-160 *Hiernaux et al.,* 2009 (Fakara area, Niger, 1994-2006) 150-230 *Mougin et al.,* 2009 (Gourma, Mali, 2005-2007)

Mass of residues (g.m^{-2})	100-300 standing in October *Schlecht et al*., 2001 (Western Niger, 1997-1998) 20-40 litter in May *Schlecht et al*., 2001 (Western Niger, 1997-1998)	
Grain yield (g.m^{-2})	40-100 *Marteau et al.,* 2011 (Niamey area, 2004-2009) 40-50 *Rockström & de Rouw,* 1997 (Banizoumbou, 1994-1996)	
Annual horizontal sediment flux (kg.m^{-1})	300-400 millet field *Abdourhamane Toure et al*., 2011 (Banizoumbou, 2007-2008) 1100-1800 bare soil *Abdourhamane Toure et al*., 2011 (Banizoumbou, 2007-2008)	2-20 *Rajot et al*., 2001 (Banizoumbou, 1996-1998)

Table 6: Observations of vegetation mass and horizontal sediment flux, from literature mostly dedicated to southwestern Niger

Our results show that realistic sets of practices have as large an influence as the largest theoretical range of practices on the variability of annual horizontal sediment flux. They induced a variability of annual horizontal sediment flux as large as that due to meteorological conditions. This study goes one step further than the benchmark study of *Pierre et al.* (2018) that addressed one land management practice at a time, considering the largest range of variation for each practice. Here, we considered scenarios representing a combination of land uses over the landscape with realistic proportional areas and associated land management practices. The practices associated with each land use within a scenario ensured internal consistency (e.g. sowing density related to soil fertility, livestock pressure related to forage availability) as land management operates in agro-pastoral systems. Off-farm activities were implicitly taken into account as they might provide income for producers to purchase fertilizers (like in '*Very high density, Intensive'*).

In future research, improvements could be brought to the simulations. For example, to explicitly account for wind erosion feedbacks on soil nutrients, dust emissions (spatially exported from the landscape) should be estimated, and spatial interactions of aeolian fluxes between land units should be taken into account, like fallows trapping part of the horizontal sediment flux from neighboring plots (*Bielders et al.,* 2004). Such estimates of sediment redistribution (i.e. budget between loss and deposition among surface types) due to wind erosion at the landscape scale would be highly valuable for assessing the dynamics of soil fertility. Similarly, trees and shrubs could be taken into account for their effect on wind erosion. As shown by *Leenders et al.* (2016), for a well-instrumented study site in Burkina Faso, shrubs

usually decrease wind erosion in their lee and increase it on their sides, with a net decreasing effect, while trees increase wind speed and thus wind erosion around their trunk.

Some uncertainties in our simulations may derive from the depiction of crop residue management in the prospective scenarios (e.g. rates of crop residues collection, constant grazing pressure throughout the dry season). Simulated practices inside a given village could exhibit a range of values instead of a unique one (e.g. rate of residues collection, dates of sowing and clearing, …; see e.g. *Raynaut,* 2001). Spatial and seasonal variability of grazing (*Turner et al.,* 2005) could also be accounted for in spatially explicit simulations, although such information is especially challenging to assess. Accordingly, the submodels for dry vegetation carry uncertainties in dry vegetation amounts, as observations used to calibrate them are very rarely available. Their improvements would require extensive measurements of both dry vegetation amounts and livestock grazing and trampling, with a good spatial and temporal coverage.

Finally, a step forward will be to run new simulations with climate conditions from past measurements and from climate projections to combine land management dynamics with regional climate change and local meteorological conditions over the long term. Climate projections to 2100 for the Sahel suggest a broad increase in temperature (*Roehrig et al.,* 2013), opposite trends in annual rainfall between western (decrease) and central and eastern (increase) Sahel, a later monsoon onset (*Monerie et al.,* 2020), and more intense rain events. These trends are associated with changes in the regional circulation, e.g. a stronger Saharan heat low (a near-surface thermal low pressure system) which affects the strength of the monsoon flow (*Parker et al.,* 2005) and could further favor the occurrence of intense mesoscale convective systems which produce wind gusts (*Fitzpatrick et al.,* 2020). As suggested by our results, these changes in meteorological conditions will affect vegetation cover and wind erosion, thus the impacts of wind erosion on the productive potential of Sahelian landscapes will be strongly influenced by future land management. The strong correlation that we noticed between horizontal sediment flux and the occurrence of strong winds recalls the fact that climate models must reproduce the occurrence and the intensity of the strongest winds in order to assess the impacts of climate change on future wind erosion.

5. Conclusion

Wind erosion has been simulated for a study site in southwestern Niger for four scenarios describing typical agro-pastoral practices of the past and future decades (1950s, 1990s, and 2030s). These scenarios focus on the dynamics of practices that are related to population increase, cropland expansion and possible future intensification. Our results clearly illustrate how evolving land use and associated management practices can affect horizontal airborne sediment flux. They underline the larger horizontal sediment flux for croplands compared to rangelands and fallows, and the importance of crop residue

management for controlling soil and nutrient losses from Sahelian agro-pastoral systems. Other factors like manuring and related crop density also produced noticeable differences in horizontal sediment fluxes among scenarios.

Our results show that land use and management changes in the study area from the 1950s to the 1990s increased aeolian sediment transport rates and are likely to continue to increase wind erosion in the coming decades. The two prospective scenarios for the 2030s exhibited similar horizontal sediment fluxes, but much larger vegetation yields under intensification (relying on external inputs and a tight crop-livestock integration) than for extensive conditions. Such a large increase of wind erosion in the coming decades would induce noticeable soil loss and associated nutrient loss, and thus ultimately a decrease in soil fertility. This land degradation would become increasingly difficult to counterbalance using fertilizers, the use of which, in addition, requires financial resources. Thus, these results bring to question the sustainability of both prospective scenarios for the 2030s.

These conclusions are particularly valuable as they have been developed for a set of consistent land use trajectories, from scenarios based on extensive knowledge of land use and land management practices of the study site. This study goes further than benchmark studies which considered one practice at a time and its sole range of variability, isolated from other practices. Thus, it recalls the fact that the environmental impact of land use and management practices, of which wind erosion is an aspect, must be assessed at the landscape scale in order to account for the contrasted surface types and associated land management.

Agro-pastoral practices are motivated by environmental and socioeconomic conditions under which smallholders must balance wind erosion trade-offs against millet yield and fodder production. While this study focused on the impacts of evolving practices, future research will combine both varying practices and climate conditions. Such results must be analyzed in relation to social changes to interpret the effect of land use changes and to better assess the impact of possible evolutions of agro-pastoral practices for the coming decades. Ultimately, future work will assess the feedbacks of wind erosion on land management and socioeconomic conditions. The scenarios and methodology we developed here are generalizable beyond this wind erosion study to systems-level investigations of human-environment interactions in the Sahelian area.

Acknowledgment:

The meteorological data monitored at Banizoumbou study site (Niger) were provided by the INDAAF network (Service National d'Observation "International Network to Study deposition and Atmospheric composition in Africa"; https://indaaf.obs-mip.fr/). INDAAF is funded by the INSU/CNRS, the IRD and the OSUs Observatoire Midi-Pyrénées (Université Paul Sabatier) and EFLUVE (Université Paris Est Créteil) and is part of the French Research Infrastructure ACTRIS-Fr. The author thanks the local operators, Aliko

Maman (IRD, Niamey, Niger) and Alfari Zakou for maintaining the station of Banizoumbou and the measurements and for providing high quality data since 2006. Monitoring of land use in the study area over the last decades was performed by P. Hiernaux and collaborators in the frame of the AMMA-CATCH Observatory. The authors thank E. Mougin, C. Delon and M. Grippa for providing the latest version of the STEP model, C. Baron for providing support on the use of the SarraH model, and A. De Rouw and G. Bergametti for their useful comments.

Declarations:

Funding: No funding was received for conducting this study. N. Webb was an invited scientist supported by the French MOPGA (Make Our Planet Great Again) program at iEES-Paris in November 2018.

Conflicts of interest: the authors have no competing interests to disclose.

Ethics approval: Not applicable

Consent to participate: Not applicable

Consent for publication: Not applicable

Availability of data: Not applicable

Author's contribution: All authors contributed to the study.

References:

Abdourhamane Touré, A., Tidjani, A.D., Rajot, J.L., Marticorena, B., Bergametti, G., Bouet, C., Ambouta, K.J.M., Garba, Z., 2019. Dynamics of wind erosion and impact of vegetation cover and land use in the Sahel: A case study on sandy dunes in southeastern Niger. Catena 177, 272–285. https://doi.org/10.1016/j.catena.2019.02.011

Abdourhamane Touré, A., Rajot, J.L., Garba, Z., Marticorena, B., Petit, C., Sebag, D., 2011. Impact of very low crop residues cover on wind erosion in the Sahel. Catena 85, 205–214. https://doi.org/10.1016/j.catena.2011.01.002

Akponikpè, P.B.I., Gérard, B., Bielders, C.L., 2014. Soil water crop modeling for decision support in millet-based systems in the Sahel: A challenge. Afr. J. Agr. Res. 9, 1700–1713. https://doi.org/10.5897/AJAR10.263

Baron, C., Sultan, B., Balme, M., Sarr, B., Traore, S., Lebel, T., Janicot, S., Dingkuhn, M., 2005. From GCM grid cell to agricultural plot: scale issues affecting modelling of climate impact. Phil. Trans. R. Soc. B 360, 2095–2108. https://doi.org/10.1098/rstb.2005.1741

Bergametti, G., Marticorena, B., Rajot, J.L., Chatenet, B., Féron, A., Gaimoz, C., Siour, G., Coulibaly, M., Koné, I., Maman, A., Zakou, A., 2017. Dust Uplift Potential in the Central Sahel: An analysis based on 10 years of meteorological measurements at high temporal resolution. J. Geophys. Res. Atmos. 122, 12,433-12,448. https://doi.org/10.1002/2017JD027471

Bergametti, G., Rajot, J.L., Pierre, C., Bouet, C., Marticorena, B., 2016. How long does precipitation inhibit wind erosion in the Sahel? Geophys. Res. Lett. 43. https://doi.org/10.1002/2016GL069324

Bielders, C.L., Rajot, J.-L., Michels, K., 2004. L'érosion éolienne dans le Sahel nigérien : influence des pratiques culturales actuelles et méthodes de lutte. Sécheresse 15, 19–32.

Bonfiglioli, A.M., 1990. Pastoralisme, agro-pastoralisme et retour : itinéraires sahéliens. Cahiers des Sciences Humaines, 3. La théorie en question 26, 255–266.

Breman, H., Groot, J.J.R., van Keulen, H., 2001. Resource limitations in Sahelian agriculture. Global Environ. Chang. 11, 59–68. https://doi.org/10.1016/S0959-3780(00)00045-5

Cappelaere, B., Descroix, L., Lebel, T., Boulain, N., Ramier, D., Laurent, J.-P., Favreau, G., Boubkraoui, S., Boucher, M., Bouzou Moussa, I., Chaffard, V., Hiernaux, P., Issoufou, H.B.A., Le Breton, E., Mamadou, I., Nazoumou, Y., Oi, M., Ottlé, C., Quantin, G., 2009. The AMMA-CATCH experiment in the cultivated Sahelian area of south-west Niger – Investigating water cycle response to a fluctuating climate and changing environment. J. Hydrol. 375, 34–51. https://doi.org/10.1016/j.jhydrol.2009.06.021

Chi, W., Zhao, Y., Kuang, W., He, H., 2019. Impacts of anthropogenic land use/cover changes on soil wind erosion in China. Sci. Total Environ. 668, 204-215. https://doi.org/10.1016/j.scitotenv.2019.03.015

de Rouw, A., Rajot, J.-L., 2004. Soil organic matter, surface crusting and erosion in Sahelian farming systems based on manuring or fallowing. Agr. Ecosyst. Environ. 104, 263–276. https://doi.org/10.1016/j.agee.2003.12.020

Dee, D.P., Uppala, S.M., Simmons, A.J., Berrisford, P., Poli, P., Kobayashi, S., Andrae, U., Balmaseda, M.A., Balsamo, G., Bauer, P., Bechtold, P., Beljaars, A.C.M., van de Berg, L., Bidlot, J., Bormann, N., Delsol, C., Dragani, R., Fuentes, M., Geer, A.J., Haimberger, L., Healy, S.B., Hersbach, H., Hólm, E.V., Isaksen, L., Kållberg, P., Köhler, M., Matricardi, M., McNally, A.P., Monge-Sanz, B.M., Morcrette, J.-J., Park, B.-K., Peubey, C., de Rosnay, P., Tavolato, C., Thépaut, J.-N., Vitart, F., 2011. The ERA-Interim reanalysis: configuration and performance of the data assimilation system. Q.J.R. Meteorol. Soc. 137, 553–597. https://doi.org/10.1002/qj.828

Du, H., Zuo, X., Li, S., Wang, T., Xue, X., 2019. Wind erosion changes induced by different grazing intensities in the desert steppe, Northern China. Agric. Ecosys. Environ. 274, 1-13. https://doi.org/10.1016/j.agee.2019.01.001

Duniway, M.C., Pfenningwerth, A.A., Fick, S.E., Nauman, T.W., Belnap, J., Barger, N.N., 2019. Wind erosion and dust from US drylands: a review of causes, consequences, and solutions in a changing world. Ecosphere 10, e02650. https://doi.org/10.1002/ecs2.2650

Fensholt, R., Rasmussen, K., Kaspersen, P., Huber, S., Horion, S., Swinnen, E., 2013. Assessing land degradation/recovery in the African Sahel from long-term Earth observation based primary productivity and precipitation relationships. Remote Sens. 5, 664–686. https://doi.org/10.3390/rs5020664

Fenta, A. A., Tsunekawa, A., Haregeweyn, N., Poesen, J., Tsubo, M., Borrelli, P., Anagos, P., Vanmaercke, M., Broeckx, J., Yasuda, H., Kawai, T., Kurosaki, Y., 2020. Land susceptibility to water and wind erosion risks in the East Africa region. Sci. Total Environ., 703, 135016. https://doi.org/10.1016/j.scitotenv.2019.135016

Fitzpatrick, R.G.J., Parker, D.J., Marsham, J.H., Rowell, D.P., Guichard, F.M., Taylor, C.M., Cook, K.H., Vizy, E.K., Jackson, L.S., Finney, D., Crook, J., Stratton, R., Tucker, S., 2020. What drives the intensification of Mesoscale Convective Systems over the West African Sahel under climate change? J. Climate 33, 3151–3172. https://doi.org/10.1175/JCLI-D-19-0380.1

Galloza, M. S., Webb, N. P., Bleiweiss, M. P., Winters, C., Herrick, J. E., Ayers, E., 2018. Exploring dust emission responses to land cover change using an ecological land classification. Aeolian Res. *32*, 141-153. https://doi.org/10.1016/j.aeolia.2018.03.001

Gomes, L., Rajot, J.L., Alfaro, S.C., Gaudichet, A., 2003. Validation of a dust production model from measurements performed in semi-arid agricultural areas of Spain and Niger. Catena 52, 257–271. https://doi.org/10.1016/S0341-8162(03)00017-1

Goutorbe, J.P., Lebel, T., Dolman, A.J., Gash, J.H.C., Kabat, P., Kerr, Y.H., Monteny, B., Prince, S.D., Stricker, J.N.M., Tinga, A., Wallace, J.S., 1997. An overview of HAPEX-Sahel: a study in climate and desertification. J. Hydrol. 188–189, 4–17. https://doi.org/10.1016/S0022-1694(96)03308-2

Greeley, R., Iversen, J.D., 1985. Wind as a geological process on Earth, Mars, Venus and Titan, Cambridge University Press. ed, Cambridge Planetary Science Series. Cambridge - London - New York - New Rochelle - Melbourne - Sydney.

Hiernaux, P., Ayantunde, A., 2004. The Fakara: a semi-arid agro-ecosystem under stress (Report of research activities), First phase (July 2002-June 2004) of the DMP-GEF Program (GEF/2711-02-4516). International Livestock Research Institute (ILRI), Niamey, Niger.

Hiernaux, P., Ayantunde, A., Kalilou, A., Mougin, E., Gérard, B., Baup, F., Grippa, M., Djaby, B., 2009. Trends in productivity of crops, fallow and rangelands in Southwest Niger: Impact of land use, management and variable rainfall. J. Hydrol. 375, 65–77. https://doi.org/10.1016/j.jhydrol.2009.01.032

Hiernaux, P., Turner, M.D., 2002. The influence of farmer and pastoralist management practices on desertification processes in the Sahel, in: Reynolds, J.F., Stafford Smith, M.D. (Eds.), Global Desertification: Do Humans Cause Deserts?, Dalhem Workshop Reports. Berlin, Germany, pp. 135–148.

IPCC, 2019: Summary for Policymakers. In: Climate Change and Land: an IPCC special report on climate change, desertification, land degradation, sustainable land management, food security, and greenhouse gas fluxes in terrestrial ecosystems [P.R. Shukla, J. Skea, E. Calvo Buendia, V. Masson-Delmotte, H.-O. Pörtner, D. C. Roberts, P. Zhai, R. Slade, S. Connors, R. van Diemen, M. Ferrat, E. Haughey, S. Luz, S. Neogi, M. Pathak, J. Petzold, J. Portugal Pereira, P. Vyas, E. Huntley, K. Kissick, M. Belkacemi, J. Malley, (eds.)]. In press.

Klein Goldewijk, K., Beusen, A., van Drecht, G., de Vos, M., 2011. The HYDE 3.1 spatially explicit database of human-induced global land-use change over the past 12,000 years. Global Ecol. Biogeogr. 20, 73–86. https://doi.org/10.1111/j.1466-8238.2010.00587.x

Kouressy, M., Dingkuhn, M., Vaksmann, M., Heinemann, A.B., 2008. Adaptation to diverse semi-arid environments of sorghum genotypes having different plant type and sensitivity to photoperiod. Agr. Forest Meteorol. 148, 357–371. https://doi.org/10.1016/j.agrformet.2007.09.009

Laurent, B., Marticorena, B., Bergametti, G., Léon, J.F., Mahowald, N.M., 2008. Modeling mineral dust emissions from the Sahara desert using new surface properties and soil database. J. Geophys. Res. 113. https://doi.org/10.1029/2007JD009484

Lavigne Delville, P., 1997. Sahelians agrarian systems: Principal rationales, in: Raynaut, C., Grégoire, E., Janin, P., Koechlin, J., Lavigne Delville, P. (Eds.), Societies and Nature in the Sahel. London, UK, pp. 138–158.

Leenders, J.K., Sterk, G., Boxel, J.H., 2016. Wind erosion reduction by scattered woody vegetation in farmers' fields in northern Burkina Faso. Land Degrad. Develop. 27, 1863–1872. https://doi.org/10.1002/ldr.2322

Marteau, R., Sultan, B., Moron, V., Alhassane, A., Baron, C., Traoré, S.B., 2011. The onset of the rainy season and farmers' sowing strategy for pearl millet cultivation in Southwest Niger. Agr. Forest Meteorol. 151, 1356–1369. https://doi.org/10.1016/j.agrformet.2011.05.018

Marticorena, B., Bergametti, G., 1995. Modeling the atmospheric dust cycle: 1. Design of a soil-derived dust emission scheme. J. Geophys. Res. 100, 16415–16430.

Marticorena, B., Chatenet, B., Rajot, J.L., Bergametti, G., Deroubaix, A., Vincent, J., Kouoi, A., Schmechtig, C., Coulibaly, M., Diallo, A., Koné, I., Maman, A., NDiaye, T., Zakou, A., 2017. Mineral dust over west and central Sahel: Seasonal patterns of dry and wet deposition fluxes from a pluriannual sampling (2006-2012). J. Geophys. Res. Atmos. 122, 1338–1364. https://doi.org/10.1002/2016JD025995

Marticorena, B., Chatenet, B., Rajot, J.L., Traoré, S., Coulibaly, M., Diallo, A., Koné, I., Maman, A., NDiaye, T., Zakou, A., 2010. Temporal variability of mineral dust concentrations over West Africa: analyses of a pluriannual monitoring from the AMMA Sahelian Dust Transect. Atmos. Chem. Phys. 10, 8899–8915. https://doi.org/10.5194/acp-10-8899-2010

Mbow, C., Brandt, M., Ouedraogo, I., De Leeuw, J., Marshall, M., 2015. What four decades of Earth observation tell us about land degradation in the Sahel? Remote Sens. 7, 4048–4067. https://doi.org/10.3390/rs70404048

Michels, K., Armbrust, D.V., Allison, B.E., Sivakumar, M.V.K., 1995. Wind and windblown sand damage to pearl millet. Agron. J. 87, 620–626. https://doi.org/10.2134/agronj1995.00021962008700040003x

Monerie, P.-A., Sanchez-Gomez, E., Gaetani, M., Mohino, E., Dong, B., 2020. Future evolution of the Sahel precipitation zonal contrast in CESM1. Clim. Dynam. 55, 2801–2821. https://doi.org/10.1007/s00382-020-05417-w

Monfreda, C., Ramankutty, N., Foley, J.A., 2008. Farming the planet: 2. Geographic distribution of crop areas, yields, physiological types, and net primary production in the year 2000. Global Biogeochem. Cy. 22, GB1022. https://doi.org/10.1029/2007GB002947

Mougin, E., Lo Seen, D., Rambal, S., Gaston, A., Hiernaux, P., 1995. A regional Sahelian grassland model to be coupled with multispectral satellite data. I: Model description and validation. Remote Sens. Environ. 52, 181–193. https://doi.org/10.1016/0034-4257(94)00126-8

Parker, D.J., Burton, R.R., Diongue-Niang, A., Ellis, R.J., Felton, M., Taylor, C.M., Thorncroft, C.D., Bessemoulin, P., Tompkins, A.M., 2005. The diurnal cycle of the West African monsoon circulation. Q. J. R. Meteorol. Soc. 131, 2839–2860. https://doi.org/10.1256/qj.04.52

Pi, H., Webb, N.P., Huggins, D.R., Sharratt, B., 2020. Critical standing crop residue amounts for wind erosion control in the inland Pacific Northwest, USA. Catena 195, 104742. https://doi.org/10.1016/j.catena.2020.104742

Pierre, C., Bergametti, G., Marticorena, B., AbdourhamaneTouré, A., Rajot, J.-L., Kergoat, L., 2014. Modeling wind erosion flux and its seasonality from a cultivated sahelian surface: A case study in Niger. Catena 122, 61–71. https://doi.org/10.1016/j.catena.2014.06.006

Pierre, C., Bergametti, G., Marticorena, B., Mougin, E., Bouet, C., Schmechtig, C., 2012. Impact of vegetation and soil moisture seasonal dynamics on dust emissions over the Sahel. J. Geophys. Res. Atmos. 117. https://doi.org/10.1029/2011JD016950

Pierre, C., Bergametti, G., Marticorena, B., Mougin, E., Lebel, T., Ali, A., 2011. Pluriannual comparisons of satellite-based rainfall products over the Sahelian belt for seasonal vegetation modeling. J. Geophys. Res. 116, D18201. https://doi.org/10.1029/2011JD016115

Pierre, C., Kergoat, L., Bergametti, G., Mougin, É., Baron, C., Abdourhamane Toure, A., Rajot, J.-L., Hiernaux, P., Marticorena, B., Delon, C., 2015. Modeling vegetation and wind erosion from a millet field and from a rangeland: Two Sahelian case studies. Aeolian Res. 19, 97–111. https://doi.org/10.1016/j.aeolia.2015.09.009

Pierre, C., Kergoat, L., Hiernaux, P., Baron, C., Bergametti, G., Rajot, J.-L., Abdourhamane Toure, A., Okin, G.S., Marticorena, B., 2018. Impact of agropastoral management on wind erosion in Sahelian croplands. Land Degrad. Develop. 29, 800–811. https://doi.org/10.1002/ldr.2783

Rajot, J.L., 2001. Wind blown sediment mass budget of Sahelian village land units in Niger. Bulletin de la Société Géologique de France 172, 523–531. https://doi.org/10.2113/172.5.523

Rakkar, M. K., Blanco-Canqui, H., Tatarko, J., 2019. Predicting soil wind erosion potential under different corn residue management scenarios in the central Great Plains. Geoderma 353, 25-34. https://doi.org/10.1016/j.geoderma.2019.05.040

Raynaut, C., 2001. Societies and nature in the Sahel: ecological diversity and social dynamics. Global Environ. Chang. 11, 9–18. https://doi.org/10.1016/S0959-3780(00)00041-8

Reenberg, A., Maman, I., Oksen, P., 2013. Twenty years of land use and livelihood changes in SE-Niger: Obsolete and short-sighted adaptation to climatic and demographic pressures? J. Arid Environ. 94, 47–58. https://doi.org/10.1016/j.jaridenv.2013.03.002

Roehrig, R., Bouniol, D., Guichard, F., Hourdin, F., Redelsperger, J.-L., 2013. The present and future of the West African Monsoon: A process-oriented assessment of CMIP5 simulations along the AMMA transect. J. Climate 26, 6471–6505. https://doi.org/10.1175/JCLI-D-12-00505.1

Schlecht, E., Kadaouré, I., Graef, I., Hülsebusch, C., Mahler, F., Becker, K., 2001. Land-use and agricultural practices in the agro-pastoral farming systems of western Niger — a case study. Die Erde 132, 399–418.

Sterk, G., 2003. Causes, consequences and control of wind erosion in Sahelian Africa: a review. Land Degrad. Develop. 14, 95–108. https://doi.org/10.1002/ldr.526

Tappan, G.G., Cushing, W.M., Cotillon, S.E., Mathis, M.L., Hutchinson, J.A., Herrmann, S.M., and Dalsted, K.J., 2016, West Africa Land Use Land Cover Time Series: U.S. Geological Survey data release, https://doi.org/10.5066/F73N21JF.

Thomas, D.T., Moore, A.D., Bell, L.W., Webb, N.P., 2018. Ground cover, erosion risk and production implications of targeted management practices in Australian mixed farming systems: Lessons from the Grain and Graze program. Agr. Syst. 162, 123–135. https://doi.org/10.1016/j.agsy.2018.02.001

Tidjani, A.D., Bielders, C.L., Ambouta, K.J.-M., 2009. Seasonal dynamics of the parameters determining wind erosion on rangeland in Eastern Niger. Geo-Eco-Trop. 33, 39–56.

Tracol, Y., Mougin, E., Hiernaux, P., Jarlan, L., 2006. Testing a sahelian grassland functioning model against herbage mass measurements. Ecol. Model. 193, 437–446. https://doi.org/10.1016/j.ecolmodel.2005.08.033

Turner, M.D., Hiernaux, P., 2015. The effects of management history and landscape position on inter-field variation in soil fertility and millet yields in southwestern Niger. Agr. Ecosyst. Environ. 211, 73–83. https://doi.org/10.1016/j.agee.2015.05.010

Turner, M.D., Hiernaux, P., Schlecht, E., 2005. The distribution of grazing pressure in relation to vegetation resources in semi-arid West Africa: The role of herding. Ecosystems 8, 668–681. https://doi.org/10.1007/s10021-003-0099-y

van Vliet, N., Reenberg, A., Rasmussen, L.V., 2013. Scientific documentation of crop land changes in the Sahel: A half empty box of knowledge to support policy? J. Arid Environ. 95, 1–13. https://doi.org/10.1016/j.jaridenv.2013.03.010

Warren, A., Batterbury, S., Osbahr, H., 2001. Soil erosion in the West African Sahel: a review and an application of a "local political ecology" approach in South West Niger. Global Environ. Chang. 11, 79–95. https://doi.org/10.1016/S0959-3780(00)00047-9

Warren, A., Osbahr, H., Batterbury, S., Chappell, A., 2003. Indigenous views of soil erosion at Fandou Béri, southwestern Niger. Geoderma 111, 439–456. https://doi.org/10.1016/S0016-7061(02)00276-8

Webb, N.P., Okin, G.S., Bhattachan, A., D'Odorico, P., Dintwe, K., Tatlhego, M., 2020. Ecosystem dynamics and aeolian sediment transport in the southern Kalahari. Afr. J. Ecol. 58, 337-344. https://doi.org/10.1111/aje.12700

Webb, N.P., Marshall, N.A., Stringer, L.C., Reed, M.S., Chappell, A., Herrick, J.E., 2017. Land degradation and climate change: building climate resilience in agriculture. Front. Ecol. Environ. 15, 450–459. https://doi.org/10.1002/fee.1530

Zhang, H., Fan, J., Cao, W., Harris, W., Li, Y., Chi, W., Wang, S., 2018. Response of wind erosion dynamics to climate change and human activity in Inner Mongolia, China during 1990 to 2015. Sci. Total Environ. 639, 1038-1050. https://doi.org/10.1016/j.scitotenv.2018.05.082

APPENDIX A: Grazing pressure for the High density (1990s) scenario

i) Forage amount:

Values (in kg of dry matter per ha) are adapted from *Hiernaux & Ayantunde* (2004; Tab. 24, 28, 29).

Herbaceous mass	yields	Palatable prop.	Palatable mass	Land use prop. in 1990s scenario	Potential livestock intake (kgDM.ha^{-1})
Rangelands	300	75%	225	20%	45
Fallows	1500	65%	975	27%	263
Manured fields	Stems: 1650 Leaves: 1350 Weeds: 250	10% 90% 50%	1505	8%	120
Unmanured fields	Stems: 1200 Leaves: 600 Weeds: 500	10% 90% 50%	910	45%	410
Leaf mass from woody plants					
Rangelands	534	20%	107	20%	21
Fallows	300	35%	105	27%	28
Fields	220	35%	77	53%	41

Table A1: Forage amounts and livestock intake at the study site in the 1990s

The total potential livestock intake is thus 928 kg.ha^{-1}. This value is in good agreement with values reported for October in Table 31 (*Hiernaux and Ayantunde*, 2004). We approximate to 0.9 t ha^{-1}, i.e. 90 t.km^{-2}, and assume that livestock can eat only about a third of it, i.e. about 30 t.km^{-2}, because of accessibility and browsing efficiency.

Yet, this palatable forage is highly variable year to year, by up to a factor 3. This value of 30 t.km^{-2} is a pluriannual average, but can thus vary every year between 15 and 45 t.km^{-2}. As livestock density does not change so largely from year to year, but over longer timescales, we take this variability into account by performing the following computation using the minimum palatable mass, i.e. 15 t.km^{-2}.

ii) Required amount per Tropical Livestock Unit (TLU):

The intake is 73g.day^{-1}.kg^{-1} of metabolic weight, where the metabolic weight is calculated as the power 0.75 of the live weight (*Assouma et al.,* 2018). Thus,

1 cattle TLU (250 kg Live weight) = 62.9 kg of metabolic weight so needs a daily intake of 4.59 kg;

Over the 9 months' dry season it corresponds to 1260 kg of forage, and to 1675 kg over 12 months.

Similarly:

1 sheep TLU (10 sheep of 25kg) = 111.8 kg metabolic weight so its daily intake is 8.162 kg;

Over the 9 months' dry season 2240 kg, and 2979 kg over 12 months.

And:

1 goat TLU (12.5 goats of 20 kg) = 118.2 kg metabolic weight so its daily intake is 8.630 kg;

Over the 9 months' dry season 2369 kg, and 3150 kg over 12 months.

Thus, if livestock is accounted for in TLU, forage intake depends on its composition. In the study area, we estimate the livestock composition in the 1990s to be 85% cattle, 10% sheep, and 5% goats in metabolic weight. Thus, the mean intake by TLU is:

0.85*1.26+0.1*2.24+0.05*2.369=1.413 t for the 9 months' dry season

0.85*1.675+0.1*2.979+0.05*3.150=1.879 t over the whole year.

Nota: In the SarraH model, livestock density can only be quantified as total TLU.km^{-2} (the livestock composition is not explicitly parameterized).

iii) Livestock density:

By comparing the available forage amount to the required intake per TLU, one estimates the grazing pressure of the study site:

15 t.km^{-2} / 1.9 t = 8 TLU.km^{-2}

This result is in good agreement with values reported in Table 35 (*Hiernaux and Ayantunde*, 2004) that yield a weighted mean of 7.7 TLU.km^{-2}. Therefore, we define a grazing pressure of 8 TLU.km^{-2} for the *High density* scenario.

References:

Assouma MH, Lecomte P, Hiernaux P, Ickowicz A, Corniaux C, Decruyenaere V, Diarra AR and Vayssières J 2018. How to better account for livestock diversity and fodder seasonality in assessing the fodder intake of livestock grazing semi-arid sub-Saharan Africa rangelands. Livestock Science 216, 16-23.

APPENDIX B: Dry season millet submodel

The submodel estimating millet masses during the dry season has been presented in *Pierre et al.* (2015). It relies on the use of additional state variables for crop residues (the masses of standing dry stems, standing dry leaves, stem litter, and leaves litter) to simulate the dynamics of dry vegetation under biotic and abiotic factors. A set of differential equations describes how each of these masses is collected, trampled, grazed, and fueled by another (e.g. when standing residue become litter). These equations use a set of calibration parameters gathered in Table B1.

In this study, the submodel has been updated based on thorough comparisons to the few available observations of the dynamics of millet residues (*Abdourhamane Toure et al.,* 2011; *Hiernaux and Ayantunde,* 2004; *Hiernaux et al.,* 2019; *Schlecht et al.,* 2001), in order to be adapted to a wide range of grazing pressure values.

	Factor	Parameter	Value (in d^{-1})	Comment
Standing vegetation	Abiotic factors	K_N Up	0.001	Same for leaves and stems
	Trampling	K_T Up	0.0006*GP	Same for standing residues and for litter Same for leaves and stems
	Intake	K_I Up Leav	0.0005*GP	Only leaves are considered palatable, not stems Same for standing leaves and litter leaves
Litter	Abiotic factors	K_N Lit	0.0147	Same for leaves and stems
	Trampling	K_T Lit	0.0006*GP	Same for standing residues and for litter Same for leaves and stems
	Intake	K_I Lit Leav	0.0005*GP	Only leaves are considered palatable, not stems Same for standing leaves and litter leaves

Table B1: Parameters used in the dry season submodel for millet masses. GP stands for Grazing Pressure (in Tropical Livestock Unit per km²)

References

Hiernaux P., Adamou K., Garba S., 2019. Notes sur la dynamique des pailles et chaumes en saison sèche 2018-2019. Observatoire AMMA-CATCH, Pastoc, Caylus, France. 15p.

APPENDIX C: Parameterizations of surface characteristics

In both cases (herbaceous and millet), the lowest possible aerodynamic roughness length is the one of the bare soil, which was determined from field measurements (z_{0s} = 9.7 10^{-5} m; *Pierre et al.,* 2015).

For herbaceous :

a) The fractional cover of grass is computed as in *Pierre et al.,* 2015:

$$f_{cvg} = 1 - e^{-0.431\ LAI_g} \quad \text{for green grass} \quad \text{(C1)}$$

$$f_{cvs} = (1 - e^{-0.9\ LAI_s})\ \frac{LAI_s}{LAI_t} \quad \text{for standing dry grass} \quad \text{(C2)}$$

$$f_{cvl} = 0.05 \ln(1 + \frac{BM_l}{28}) \quad \text{for dry litter grass} \quad \text{(C3)}$$

Where LAI_g, LAI_s, LAI_t are respectively the LAI for green, standing dry and total grass cover.

b) $z_0 = 0.0003 * BM_{std} + 0.0007 * BM_{lit}$ (C4)

with BM_{std} (mass of standing herbaceous) and BM_{lit} (mass of litter herbaceous) in g.m^{-2} and z_0 in m.

For millet:

a) At the beginning of plant growth (from germination to the beginning of the reproductive stage) the vegetation mass simulated in SarraH (M_{tot}) is underestimated (*Pierre et al.,* 2018). The corrected vegetation mass ($M_{tot\ cor}$) is computed as a linear interpolation of M_{tot} for this part of the year.

b) The fractional cover of green and dry standing millet $f_{cv\ std}$ is computed as

$f_{cv\ std} = 1 - e^{-0.45\ LAIstd}$ (C5)

whith LAI_{std} the LAI of green and dry standing millet.

The fractional cover of litter millet is computed as

$f_{cv\ lit} = (0.14\ BM_{lit} + 0.23)/100$ (C6)

where: BM_{lit} is the litter mass of millet (in $g.m^{-2}$).

The total fractional cover f_{cv} is the sum of $f_{cv\ std}$ and $f_{cv\ lit}$. Finally, the erodible surface ration is $E=1-f_{cv}$.

c) For standing millet:

$$z_0 = 0.00036\ BM_{tot\ cor} \qquad \text{(C7)}$$

where: $BM_{tot\ cor}$ is in $g.m^{-2}$ and z_0 is in m and cannot exceed 10 cm.

For litter millet:

$$z_0 = 0.0012\ \ln(f_{cv\ lit}) + 0.0013 \qquad \text{(C8)}$$

when only litter is present (from field clearing to the following germination). At the beginning of plant growth, the new vegetation is still very small and would result in a low surface roughness, whereas litter may remain from the previous growing year, possibly inducing a larger surface roughness. Therefore, z_0 is calculated as the maximum of Equations C7 and C8 during this period.

APPENDIX D: Variability of the annual horizontal flux

Scenario	Mean over years	Std over years	std/mean over years
Low density	0	0	/
High density	176	186	1.05
Very high density, Extensive	519	412	0.79
Very high density, Intensive	452	317	0.70
Bare soil	*830*	*426*	*0.51*

Table D1: Variability of the annual horizontal sediment flux (in kg.m^{-1}) over years for each scenario

Year	2006	2007	2008	2009	2010	2011	2012	2013	2014	2015	2016	2017
Mean of scenarios	591	685	585	255	445	163	161	179	158	113	82	29
Std of scenarios	510	532	460	200	398	158	160	166	141	100	89	27
Std/mean	0.86	0.78	0.79	0.79	0.89	0.97	0.99	0.93	0.89	0.89	1.09	0.94
Prop wind > 7 m.s^{-1} (%)	*2.24*	*2.29*	*2.08*	*1.41*	*1.68*	*1.35*	*1.52*	*0.84*	*0.68*	*0.98*	*0.54*	*0.59*

Table D2: Variability of the annual horizontal sediment flux (in kg.m^{-1}) over scenarios for each year, and proportion of large winds